NJIT
New Jersey's Science & Technology University

University of Mississippi

FLOOD MITIGATION ENGINEERING RESOURCE CENTER (FMERC) - PROJECT EC14-005

18 June, 2014

Final Report Appendix E- Oradell Dam Break Simulation Analysis (Section 3.5 in Final Report)

Submitted to:

NEW JERSEY DEPARTMENT OF ENVIRONMENTAL PROTECTION
Office of Engineering and Construction
Trenton, NJ
Attn: Dave Rosenblatt, Administrator
John Moyle, Manager of Dam Safety and Flood Control

1. Introduction

The Oradell Dam is a 22-foot high concrete dam located on the Hackensack River in Bergen County, New Jersey. The Oradell dam was built in 1901 by the dredging of a mill pond. In 1911 the mill pond was replaced by a timber-crib dam to increase storage. The construction of a 22-foot high concrete gravity dam to further increase storage began in 1921 and was completed in 1923.

The Oradell Reservoir has a normal storage volume of 10,740 acre-feet at elevation 22.2 ft NAVD 88. The surface area at normal storage is 796 acres. Maximum storage volume is 13,316 acre-feet at elevation 24.68 ft NAVD 88, which is also the crest elevation of the dam. The hydraulic height of the dam is 25 ft. The reservoir provides drinking water to a population of about 750,000 living in Bergen and Hudson counties[1]. The reservoir provides drinking water to a population of about 750,000 living in Bergen and Hudson counties.

This section analyzes the consequences of the hypothetical failure of the Oradell Dam during a major storm surge event such as the one caused by Hurricane Sandy in 2012.

2. Objectives of the Oradell Dam Break Simulation and Impact Analysis

Oradell Dam is a critical infrastructure, whose failure during a storm surge event such as Hurricane Sandy (2012) may exacerbate flooding and lead to loss-of-life and property damage. This section presents the results of the Spillway Design Flood failure of the Oradell dam during Hurricane Sandy (abbreviated DB&SS) and analyzes the consequences in terms of increase of flood extent and flooding depths with respect to two other failure simulations: 1) "Spillway Design Flood (abbreviated SDF)" failure scenario without the storm surge flooding at the downstream, and 2) "Storm Surge Only (abbreviated SSO)" scenario without the dam-breach. The initial and boundary conditions for the simulations with storm surge were taken from the base-scenario of Hurricane Sandy simulation using CCHE2D, which is described in Sections 2.2 and 2.3 of the report.

3. Description of DSS-WISE™ Model

The dam-break simulations were performed using DSS-WISE™ software developed by the National center for Computational Hydroscience and Engineering at the University (NCCHE) of Mississippi. DSS-WISE™ is an integrated software for dam-break flood analysis which includes a state of the art solver that can handle mixed flow regimes, and wetting and drying. It has a GIS-based graphical user interface and the results provided by the DSS-WISE™ are compatible with HAZUS-MH for consequence analysis.

The numerical solver of the DSS-WISE™ software solves the conservative form of shallow water equations that govern the flood propagation over complex topography. Referring to the definition sketch in Figure 1, the conservative form of shallow water equations in vector format can be written as

$$\boldsymbol{U}_t + [\boldsymbol{F}(\boldsymbol{U})]_x + [\boldsymbol{G}(\boldsymbol{U})]_y = \boldsymbol{S}(\boldsymbol{U}) \tag{1}$$

---

[1] http://en.wikipedia.org/wiki/Oradell_Reservoir
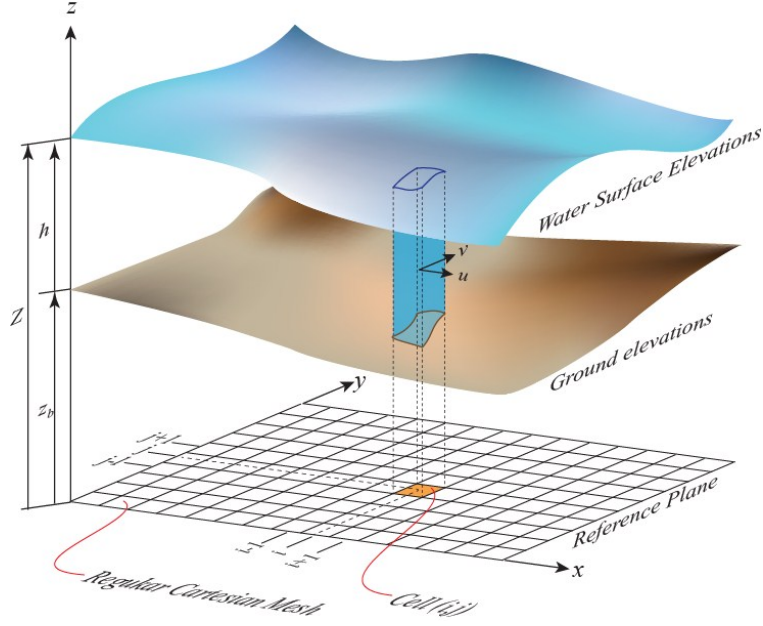
Figure 1 Definition sketch for modeling of shallow water flow over complex topography.

Bolded symbols in Figure 1 represent vectors with U being the vector of conserved variables, $F(U)$ and $G(U)$ the fluxes in x and y directions, respectively.

$$U = \begin{bmatrix} h \\ hu \\ hv \end{bmatrix} \ , \ F(U) = \begin{bmatrix} hu \\ huu + gh^2/2 \\ huv \end{bmatrix} \ , \ G(U) = \begin{bmatrix} hv \\ hvu \\ hvv + gh^2/2 \end{bmatrix} \tag{2}$$

The term on the right side of the equation, (U) , is the vector of source terms due to topography and friction.

$$S(U) = \begin{bmatrix} q_v \\ -ghS_{fx} - gh(\partial z_b/\partial x) \\ -ghS_{fy} - gh(\partial z_b/\partial y) \end{bmatrix} \tag{3}$$

In these equations, u and v are the local velocity components in x and y directions, h the flow depth, z_b the bed elevation, g the gravitational acceleration, and q_v the net source/sink discharge (or mass per cell area per unit time) added without momentum input. The system of equations is closed by assuming that the source terms due to friction, S_{fx} and S_{fy}, are expressed by the Manning's equation, in which n stands for Manning's friction coefficient:

$$\text{with } S_{fx} = \frac{u \, n^2 \, \sqrt{u^2+v^2}}{h^{4/3}} \text{ and } S_{fy} = \frac{v \, n^2 \, \sqrt{u^2+v^2}}{h^{4/3}} \tag{4}$$
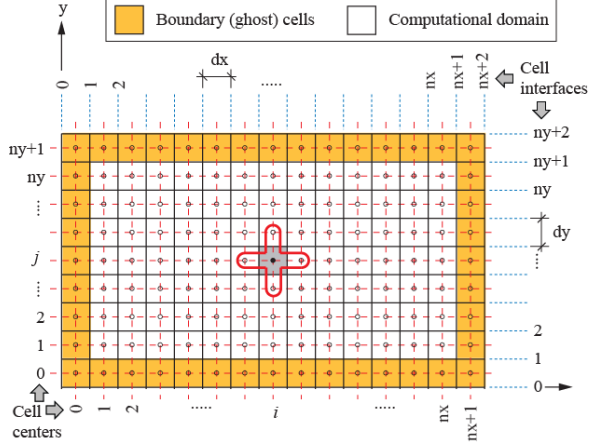
Figure 2 Regular Cartesian computational mesh used by DSS-WISE™.
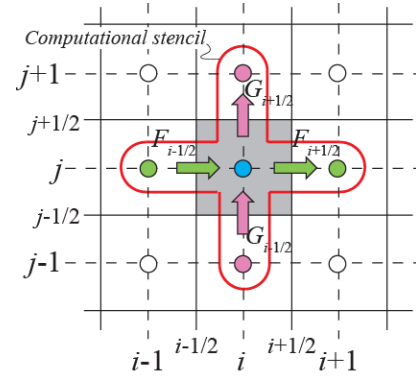
Figure 3 Computational stencil.

DSS-WISE™ assumes that the solution domain can be represented as a regular Cartesian mesh defined in x-y horizontal plane (see Figure 1 and Figure 2), such as a DEM (Digital Elevation Model). The step sizes in x and y directions are in Δx and Δy, respectively. The z axis represents elevation with respect to an arbitrary datum. Gravitational acceleration is normal to the plane and points in the negative z direction. Again referring to Figure 1, the finite volume method is used to obtain an explicit discreet time marching equation for solving the three unknowns, i.e. h, hu, and hv , by integrating the shallow water equations given in Eq. (1) over the cell (i,j):

$$U_{i,j}^{m+1} = U_{i,j}^m - \left(\frac{\Delta t}{\Delta x}\right)\left(F_{i+\frac{1}{2},j} - F_{i-\frac{1}{2},j}\right) - \left(\frac{\Delta t}{\Delta y}\right)\left(G_{i,j+\frac{1}{2}} - G_{i,j-\frac{1}{2}}\right) + \Delta t S_{i,j} \tag{5}$$

In the above equation, $F_{i+1/2,j}$ and $F_{i-1/2,j}$ express the fluxes through the east and west intercell boundaries, and $G_{i+1/2,j}$ and $G_{i-1/2,j}$ through north and south intercell boundaries, respectively (see Figure 3). Developing a robust and stable shock-capturing upwind numerical model requires the selection of appropriate expressions to compute the intercell fluxes. DSS-WISE™ adopts a Godunov (Godunov 1959 and Godunov et al. 1976) type upwind scheme based on the approximate solution of Generalized Riemann Problem (GRP) at each cell interface using the first-order HLLC Riemann solver (Toro et al., 1992, 1994). The HLLC method is a modified version of the HLL (Harten, Lax and van Leer) Riemann solver originally proposed by Harten, Lax, and van Leer (1983). The C in HLLC method stands for the contact wave (when solving equations in one direction; the variation of variables in the other direction behave as contact waves). The HLLC method offers several advantages. It is relatively simple and straightforward to implement. It does not require entropy fixes to avoid physically impossible solutions. It can handle wet-dry fronts without having to define a minimum water depth everywhere. The details of the implementation can be found in Altinakar and McGrath (2012b).

The explicit scheme used by CCHE2D-FLOOD is subjected to Courant-Friedrichs-Lewy (CFL) condition for convergence, which states that the fastest wave in the domain should only travel a fraction of the cell size ($\Delta x = \Delta y$) during the time step Δt. Based on the CFL condition, the time step is automatically chosen using the following criteria:

$$N_{CFL} = \text{Max}\left[\frac{\Delta t}{\Delta x}\left(|u| + \sqrt{gh}\right), \frac{\Delta t}{\Delta y}\left(|v| + \sqrt{gh}\right)\right] \leq 0.5 \tag{6}$$

The DSS-WISE™ is programmed using multi-core multi-threaded parallelization to increase the computational speed. It also uses special techniques to track and compute only wet cells to further increase the computational speed (Altinakar et al. 2012).

Originally developed with funding from the U.S. Department of Homeland Security (DHS) Science and Technology Directorate, the DSS-WISE™ has been extensively verified and validated using various analytical solutions and mathematical constructs. It has also been validated using field data from past dam failures (Altinakar et al. 2010). A blind validation study was also performed in collaboration with USACE MMC (Altinakar et al. 2012a). In collaboration with the Office of Infrastructure Protection, DHS National Protection and Programs Directorate, and the Office of Homeland Security, USACE Headquarters, a simplified version of DSS-WISE™, called DSS-WISE™ Lite, is currently available for web-based automated dam-break flood modeling and mapping tool through, which is accessible via DSAT (Dams Sector Analysis Tool) portal hosted by the Argonne National Laboratory (ANL).

4. Computational Conditions

The computational mesh for storm surge simulations did not include Oradell Dam and reservoir. The DEM for dam-break simulations was, therefore, created using data from different sources. Since the simulation of the hypothetical failure of Oradell Dam required initial and boundary conditions of the storm surge flood, the DEM used for the storm surge simulations was directly burned into the larger DEM used for dam-break flood simulations in order to have exactly the same conditions.

Figure 4 shows the extent of the computational meshes for the storm surge simulations (blue rectangle) and dam break simulations (red rectangle). The DEM for the area entire computational area (delineated by the red rectangle in Figure 4) was created from 1/3 arc-second USGS NED[2] (The National Elevation Dataset) tiles re-projected to 5m UTM zone 18. The mesh used in the storm surge simulation (the area covered by the blue rectangle was converted into 5m raster projected UTM zone 18 was then burned onto this DEM. The area around the Oradell Dam and Reservoir was generated from 1/9 arc-second USGS NED tiles re-projected to 5m UTM zone 18 and burned into the DEM created in the first step. The bathymetry of the channel and estimated bathymetry of the Oradell Reservoir were also burned to complete the DEM to be used for dam-break flood simulations with and without the storm surge.

The final DEM used for the simulations is shown in Figure 5. It has 6,887 columns and 8,768 rows. The total number of cells is 60,385,216. The resolution is 5m in both x (West-East) and y (South-North) directions, i.e. $\Delta x = \Delta y = 5m$.

---

[2] http://ned.usgs.gov/
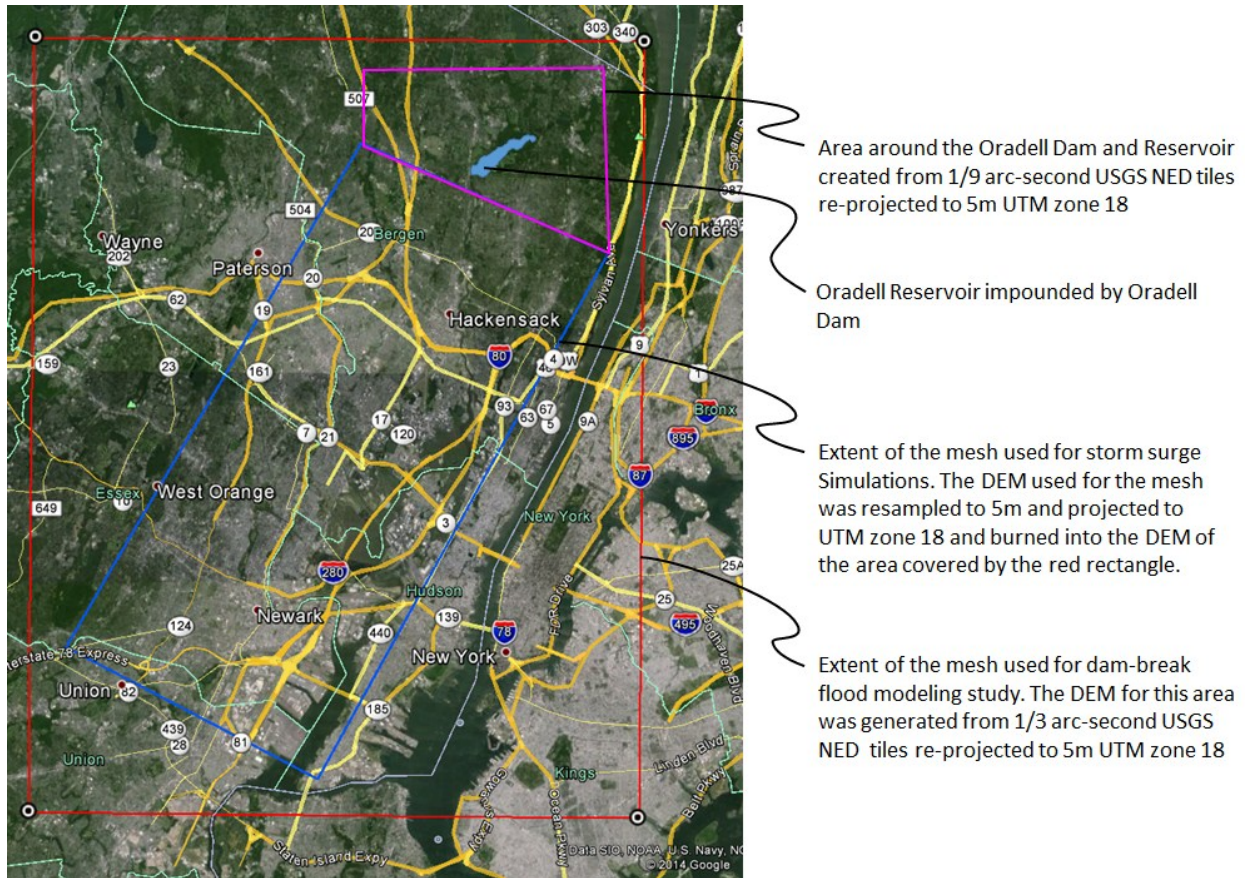
Figure 4 Comparison of the extents of the computational domains for storm surge and dam-break flood simulations.

The Manning's coefficients of friction (or Manning's roughness coefficient) for the computational cells were determined based on the land use/cover information as given in the National Land Cover Database 2006[3] (NLCD-2006) published by The Multi-Resolution Land Characteristics Consortium (MRLC)[4]. NLCD-2006 has 21 land cover classification classes (including the unclassified), which have been applied consistently across the conterminous United States at a spatial resolution of 30 meters. Figure 6 show the map of land use/cover classes for the computational domain. The 21 size classes and the corresponding Manning's roughness values are listed in Table 1. More detailed information on the description of each land use/cover class can be obtained from the MRLC website[5].

---

[3] http://www.mrlc.gov/nlcd2006.php
[4] http://www.mrlc.gov/index.php
[5] http://www.mrlc.gov/nlcd06_leg.php
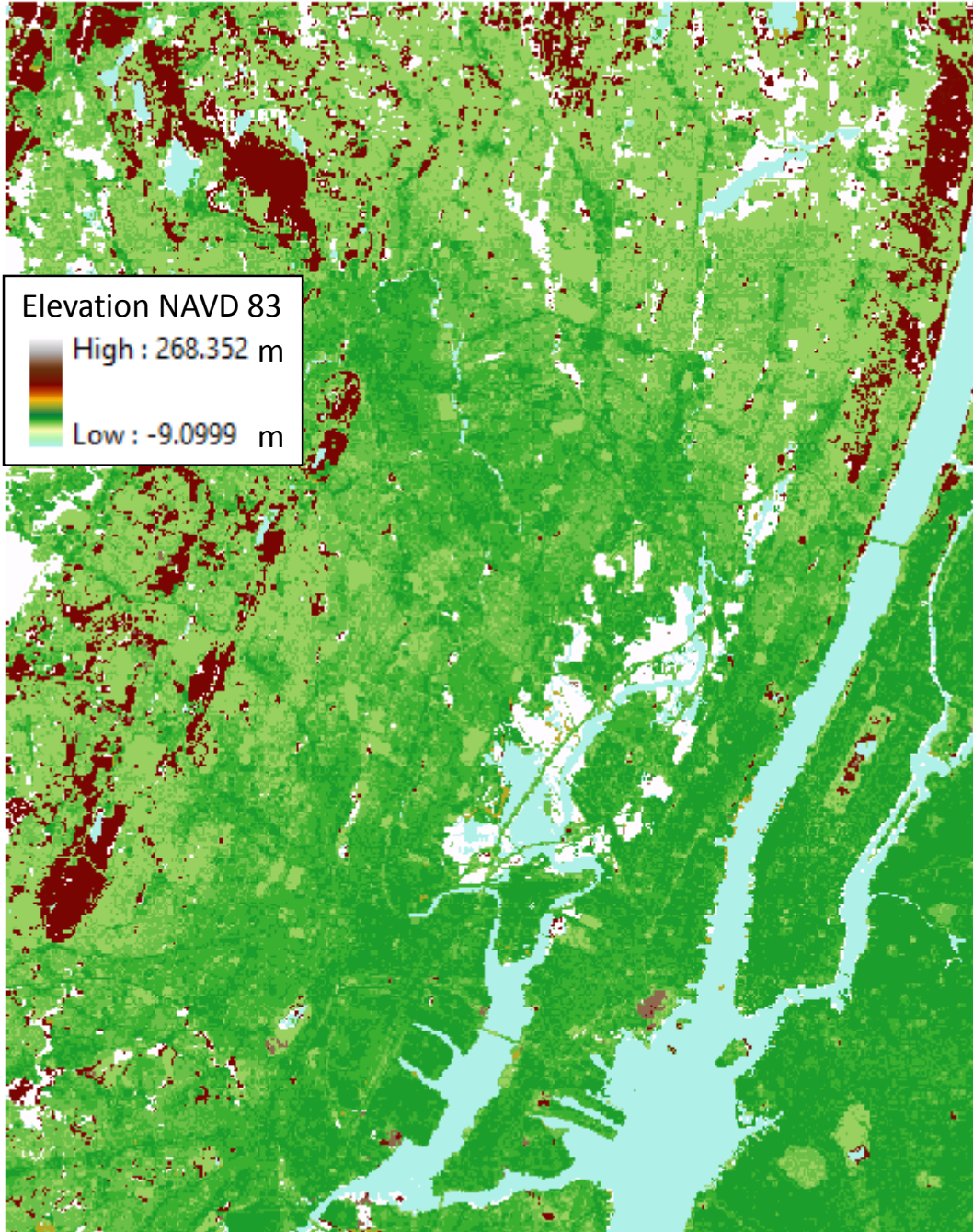
Figure 5 Digital Elevation Model (DEM), which was used as computational domain.

Figure 6 Land use classes in the computational domain (see Table 1 for the color code, description for each land use class and the corresponding Manning's n values).

Table 1 Color codes and Manning's n values for land use classes and number of cells (5m×5m) in the inundation area for each land use type.

Color	Class ID	n (m^{-1/3}s)	Description	Number of Cells in the Inundation Area		
				Sunny Day Failure	Only Storm Surge	Dam Break and Storm Surge
	0	0.0350	Unclassified			
	11	0.0330	Open Water	1,934	116,003	90,910
	12	0.0100	Perennial Snow/Ice			
	21	0.0404	Developed, Open Space	26,367	106,838	126,705
	22	0.0678	Developed, Low Intensity	23,663	266,432	292,325
	23	0.0678	Developed, Medium Intensity	25,179	563,132	607,019
	24	0.0404	Developed, High Intensity	18,629	648,528	687,942
	31	0.0113	Barren Land	104	6,033	6,103
	41	0.1000	Deciduous Forest *	982	6,213	7,007
	42	0.1000	Evergreen Forest *	3	262	262
	43	0.1200	Mixed Forest *			
	51	0.0350	Dwarf Scrub *			
	52	0.0400	Shrub/Scrub	428	5,390	5,427
	71	0.0400	Grassland/Herbaceuous	283	3,606	3,663
	72	0.0350	Sedge/Herbaceous *			
	73	0.0350	Lichens *			
	74	0.0350	Moss *			
	81	0.0350	Hay/Pasture		6,277	6,312
	82	0.0700	Cultivated Crops	484	872	1,390
	90	0.1500	Woody Wetlands	29,676	234,092	255,309
	95	0.1825	Emergent Herbaceuous Wetlands	2384	32,482	32,935

A total of eight observation lines and 25 observation points were defined to extract data as a function of time. The locations of these observation lines and points are shown in Figure 7. Observation lines provide the computed discharge hydrograph crossing the line in both directions. The positive discharge direction was chosen to point downstream along the Hackensack River. Therefore, positive discharge values in hydrograph plots at observation lines indicate a flow to downstream (towards the see), and the negative discharges correspond to a flow moving inland. Observation points provide information on local depth and local velocity components in x and y directions as a function of time.

Initial and boundary conditions for each of the three scenarios simulated in this study are described in the following section. For the simulations with the storm surge (with or without the dam break), the depth map and the maps of velocity components in x and y directions obtained from the storm surge simulation using CCHE2D (see Sections 2.2 and 2.3 of the report) were used as initial conditions.
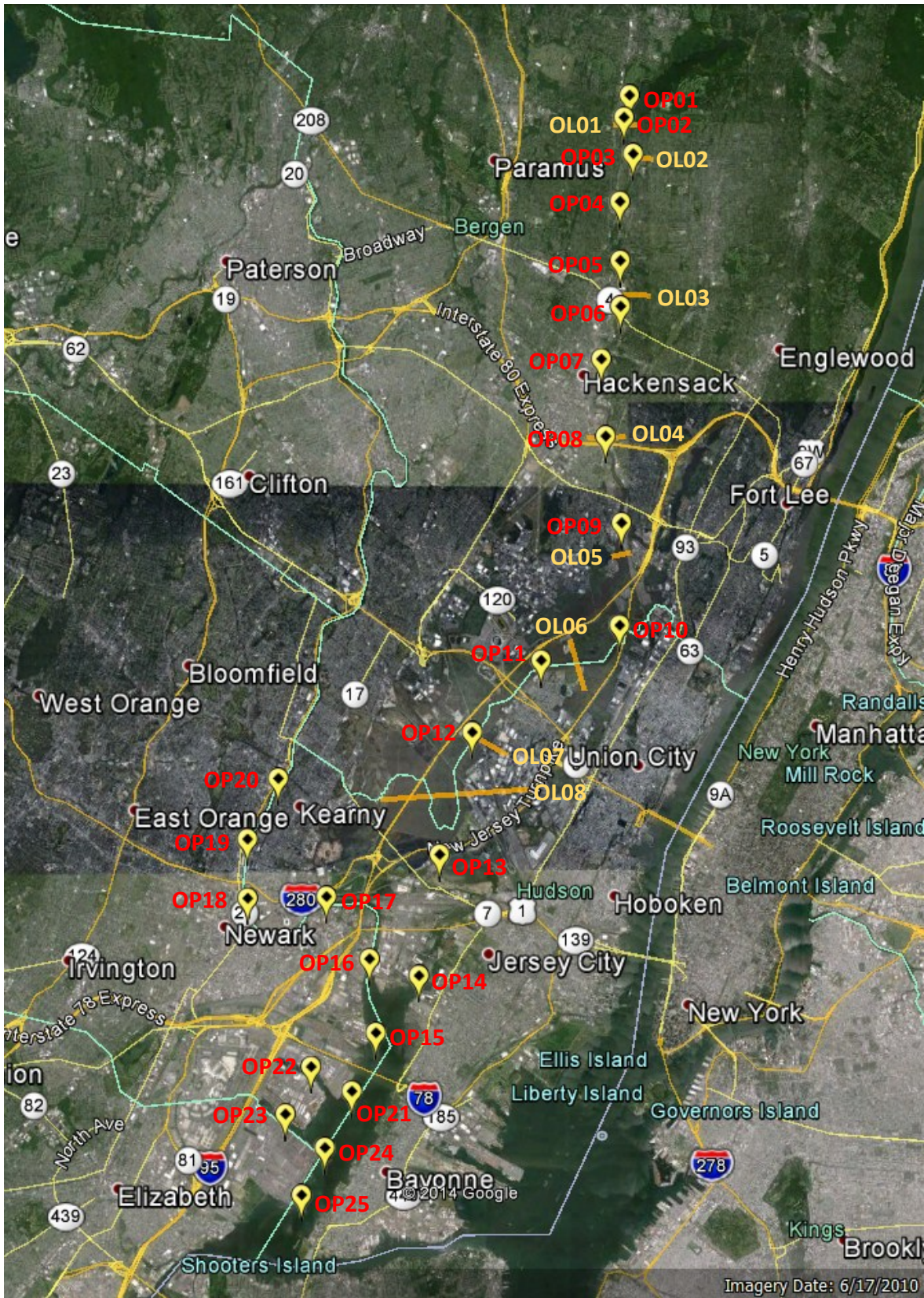
Figure 7 Google Earth map showing the locations of observation points and lines.

5. Description of the Simulated Scenarios

The three scenarios simulated for Oradell Dam are described below:

Spillway Design Flood (abbreviated as SDF): For the failure scenario of Spillway Design Flood, the downstream floodplain was assumed to be completely dry. Only a constant water surface elevation of 1.175m (NAVD 88) was assumed in the downstream channel and bay. This value corresponds to high tide value at 407,160 s in the base scenario of storm surge simulations.

The spillway design flood for Oradell Dam is the 0.3 PMF event based on the Owner's consultant. The 0.3 PMF event produces a peak water surface elevation of approximately 29 ft NGVD 29, which was assumed to be the initial water surface elevation for the simulation.

Oradell Dam is a concrete dam. There are no standard guidelines for selecting the breach width and formation time for concrete dams. The following values were assumed based on the information received from New Jersey Department of Environmental Quality (NJDEP):

Pool elevation at failure: 28.01 ft NAVD 88 (29.0 ft NGVD 29)
Storage volume at failure: 15,756 acre-ft
Final Breach Width: 200 ft (corresponds to about six out of 11 blocks failing together)
Breach Formation Time: 0.1 hrs (USACE MMC recommends a short time for concrete dam failure)
Breach Invert Elevation: 2.67 ft NAVD 88

It was assumed that the dam breaches at the beginning of the simulation (t = 0 s). The simulation was computed for 24 hours of flood time and it took 3 hours and 52 minutes of wall time to complete on a desktop computer with 16 processors. At the end of the simulation 1,444,479 cells (5m×5m) were containing water.

Storm Surge Only (abbreviated as SSO): This scenario simulates the storm surge for the base scenario of Hurricane Sandy during a three day period extending from 22:00hr on 10/29/2012 to 22:00hr on 11/1/2012. The beginning of the simulation (1,288,800 s) is at about 3 hours 24 minutes before the peak surge tide, which occurs at 1,301,040 s (i.e. at 1:24hr on 10/30/2012).

The initial conditions at the beginning of the simulations were taken from the results of the base scenario of Hurricane Sandy simulated using CCHE2D-Coast software ("Frame 23" in the history file). These included the water surface map and velocity components in x and y directions. CCHE2D-Coast uses a structured, non-orthogonal finite element mesh with variable element sizes. It was therefore necessary to resample the results computed with CCHE2D-Coast into 5m raster projected with UTM zone 18. Since small differences in ground elevation may exist between the mesh used by CCHE2D and DSS-WISE™, the depth grid was obtained by subtracting the DEM from the rasterized water surface elevation. In addition, a discharge hydrograph was imposed immediately downstream of the Oradell Dam in the same way as it was done in storm surge base scenario. The time variation of the water surface elevation along the south boundary of the CCHE2D-Coast mesh during the three day simulation period was imposed as downstream boundary condition.

The simulation was computed for 3 days and it took 2 days 12 hours wall time to complete on a desktop computer with 16 processors while other jobs were also running. At the end of the simulation, 3,834,361 computational cells (5m×5m) were containing water.
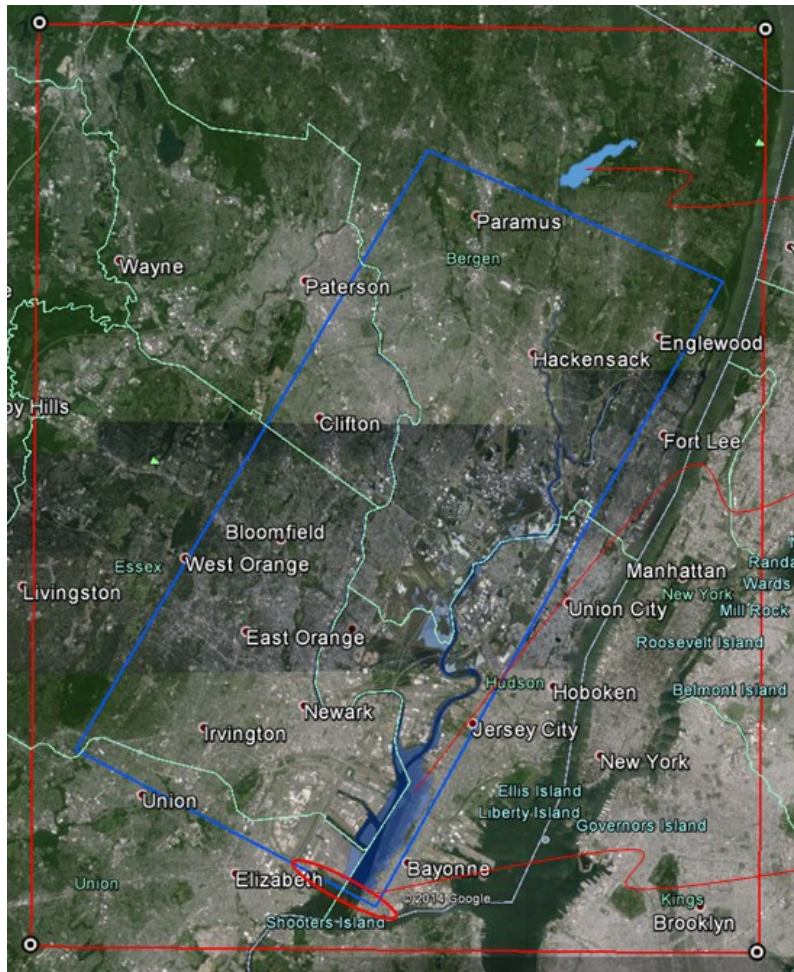
Initial conditions for DB&SS simulation included the Oradell reservoir with a water surface elevation of 28ft NAVD 83. The discharges released from the dam prior to the failure was imposed as a known hydrograph.

Initial conditions (water depths and velocity components in x and y directions) for SSO and DB&SS simulations were taken from the Hurricane Sandy base-scenario simulation with CCHE2D-Coast.

Time variation of the waters surface elevation computed during Hurricane Sandy base-scenario simulation with CCHE2D-Coast was imposed as boundary condition for the simulations with scenarios SSO and DB&SS.

Figure 8 Initial conditions and boundary conditions for the scenarios SSO and DB&SS.

Dam-Break Failure during Storm Surge (abbreviated as DB&SS): This scenario simulates the dam-break during the base scenario of Hurricane Sandy. The time period is the same as the one used in SSO. The three-day simulation begins at 22:00hr on 10/29/2012, approximately 3 hours before the peak surge tide, and terminates at 22:00hr on 11/1/2012.

The initial and boundary conditions related to storm surge are the same as for the scenario SSO. The failure conditions for the Oradell Dam are the same as for the scenario SDF. The simulation begins at 1,288,800 s corresponding to 22:00hr on 10/29/2012. The Oradell Dam is breached at 1,290,240 s (22:24hr on 10/29/2012), which is 24 minutes after the beginning of the simulation. The initiation of the breach is timed to occur three hours before the peak of the surge tide, which occurs at 1,301,040 s (i.e. at 1:24hr on 10/30/2012).

The simulation was computed for 3 days and it took 1 day 19 hours wall time to complete on a desktop computer with 16 processors. At the end of the simulation, 4,135,474 computational cells (5m×5m) were containing water.

The results files provided by the DSS-WISE™ include:
- Raster file of maximum flood depths, h_{max}, in meters,

- Raster file of flood arrival time, t_{arr}, in seconds with respect to a prescribed time origin,
- Raster file of maximum flood discharges per unit width, q_{max}, in $m^3/s/m$,
- Raster file of flood depths (in meters) at the end of the simulation,
- Raster file of flood velocity in x direction, u (in m/s) at the end of the simulation,
- Raster file of flood velocity in y direction, v (in m/s) at the end of the simulation,
- A comma separated value (csv) file for each observation line, and
- A comma separated value (csv) file for each observation point.
- A KMZ file for visualizing the results on Google Earth

All raster files can be directly imported into ArcGIS or any other GIS software. All raster files are compatible with HAZUS-MH.

The comma separated value files for observation lines contain data in five columns: (1) time in seconds (data was recorded at 10 minute intervals), (2) discharge (in m^3/s) in positive direction, (3) discharge (in m^3/s) in negative direction, (4) length (in m) of the observation line along which the discharge is in positive direction, and (5) length (in m) of the observation line along which the discharge is in negative direction.

The comma separated value files for observation points contain data in five columns: (1) time in seconds (data was recorded at 10 minute intervals), (2) flow depth (in m), (3) flow velocity (in m/s) in x direction, (4) flow velocity (in m/s) in y direction, and (5) bed elevation (in m NAVD 88).

6. Results of the Simulations

6.1. Spillway Design Flood Failure Simulation (SDF)

Figure 9 shows the maximum depth raster for the scenario SDF.
Figure 10 shows the flood arrival time raster for the scenario SDF.
Figure 11 shows the maximum flood discharge per unit width for the scenario SDF.

The discharge hydrographs computed at observation lines 1, 3, 4, 5, 6, 7, and 8 are plotted together in Figure 12. The maximum discharge of 693m^3/s is observed at OL-01 at 0.233 hours after the initiation of the breach. The discharge at OL-01 rises very quickly but decays more slowly. The peak discharges of hydrographs decrease with downstream distance from the dam due to attenuation and the rise time of the hydrograph increases.
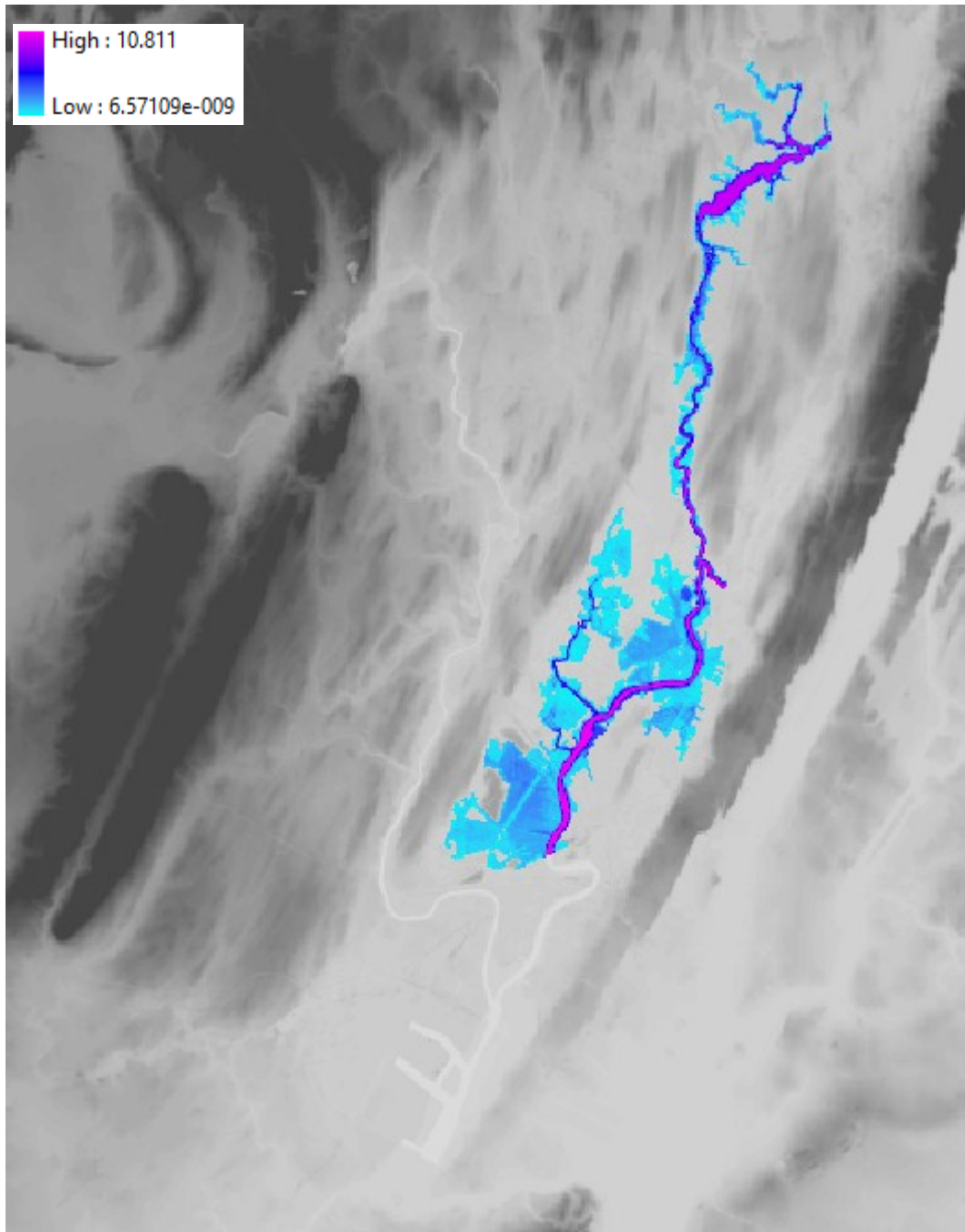
Figure 9 Map of maximum flow depths for the Spillway Design Flood failure scenario (SDF). The units for the legend are in meters.
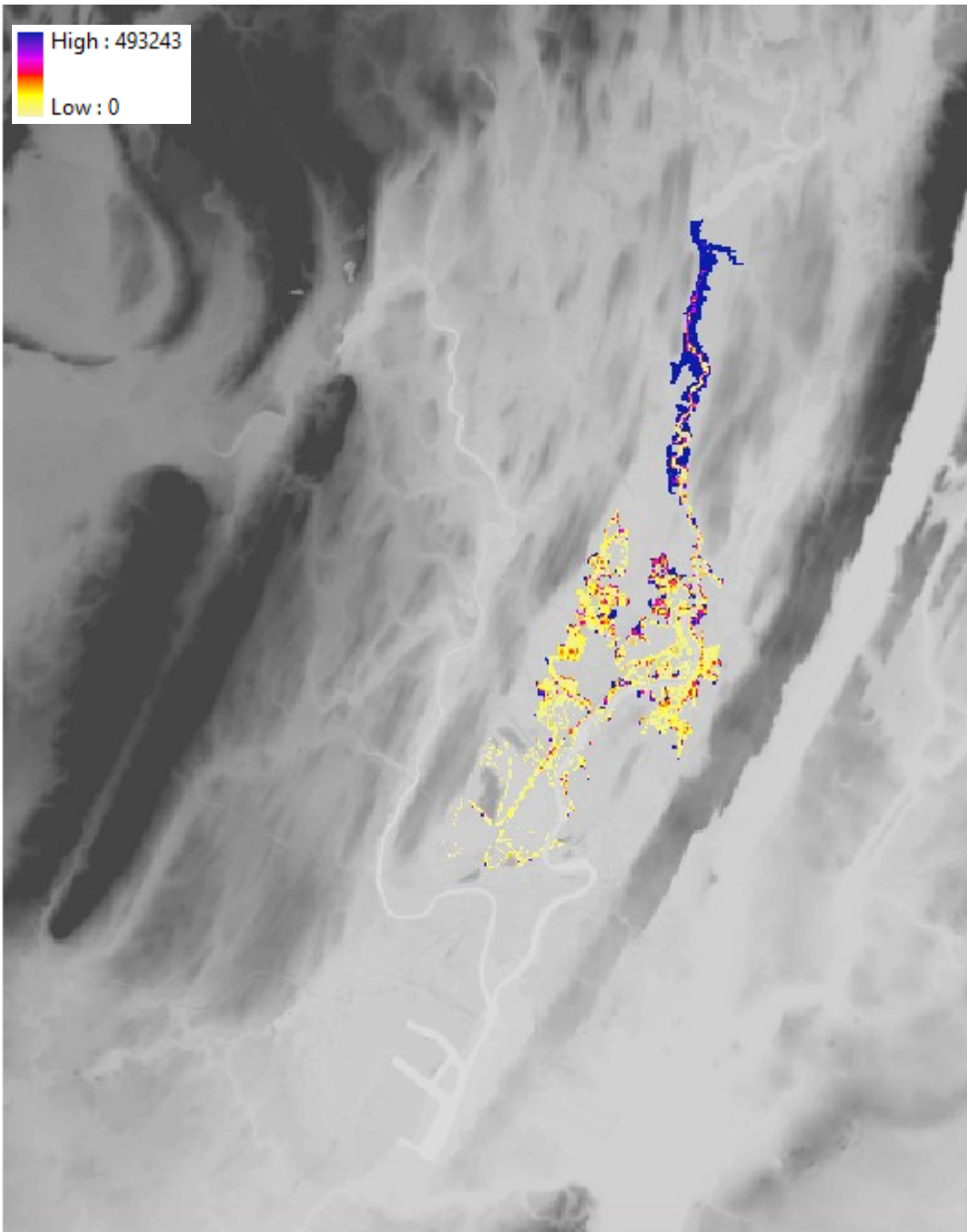
Figure 10 Map of flood arrival times for the Spillway Design Flood failure scenario (SDF). The units for the legend are in seconds.
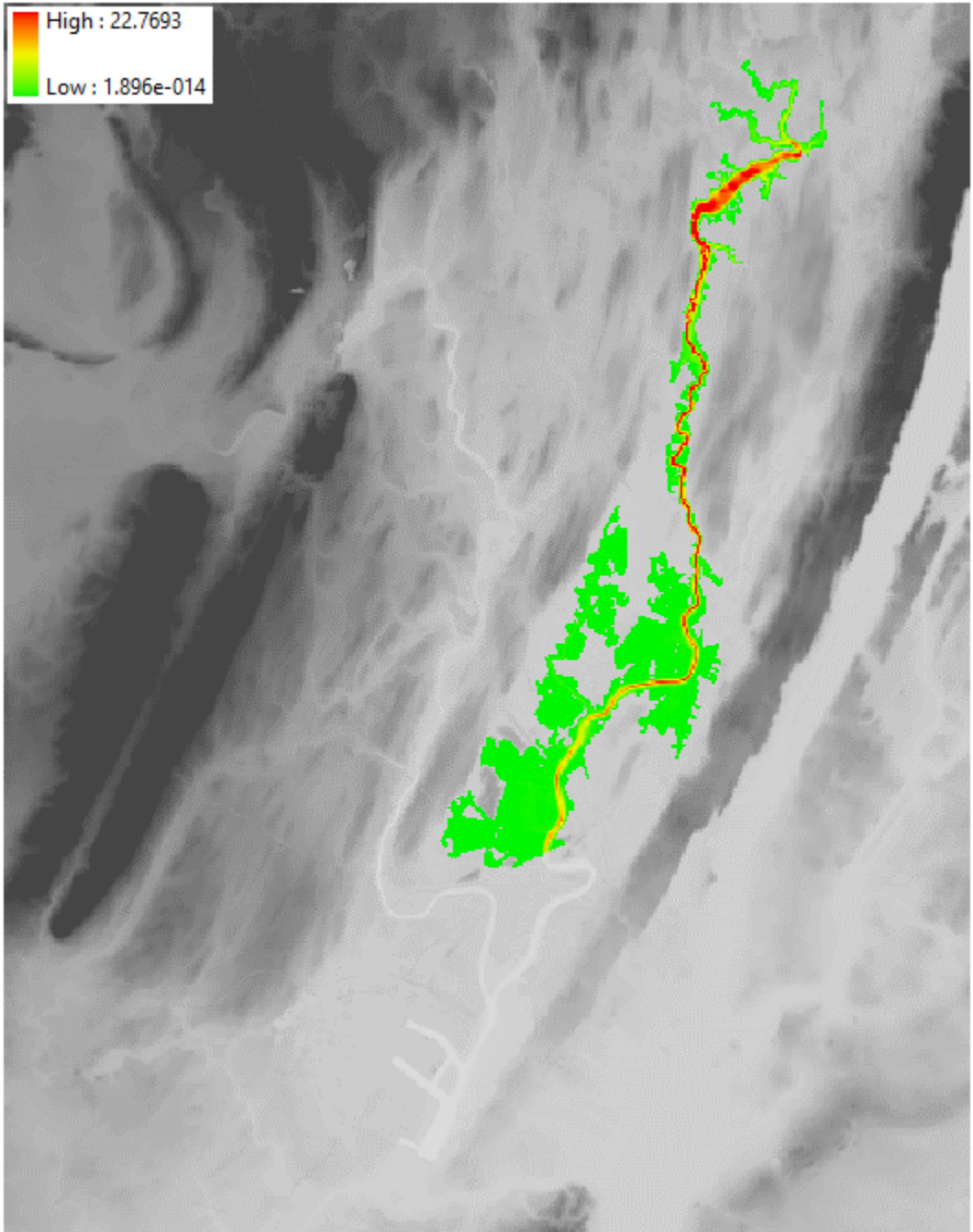
Figure 11 Map of maximum flow discharge per unit width for the Spillway Design Flood failure scenario (SDF). The units for the legend are in m^3/s/m.
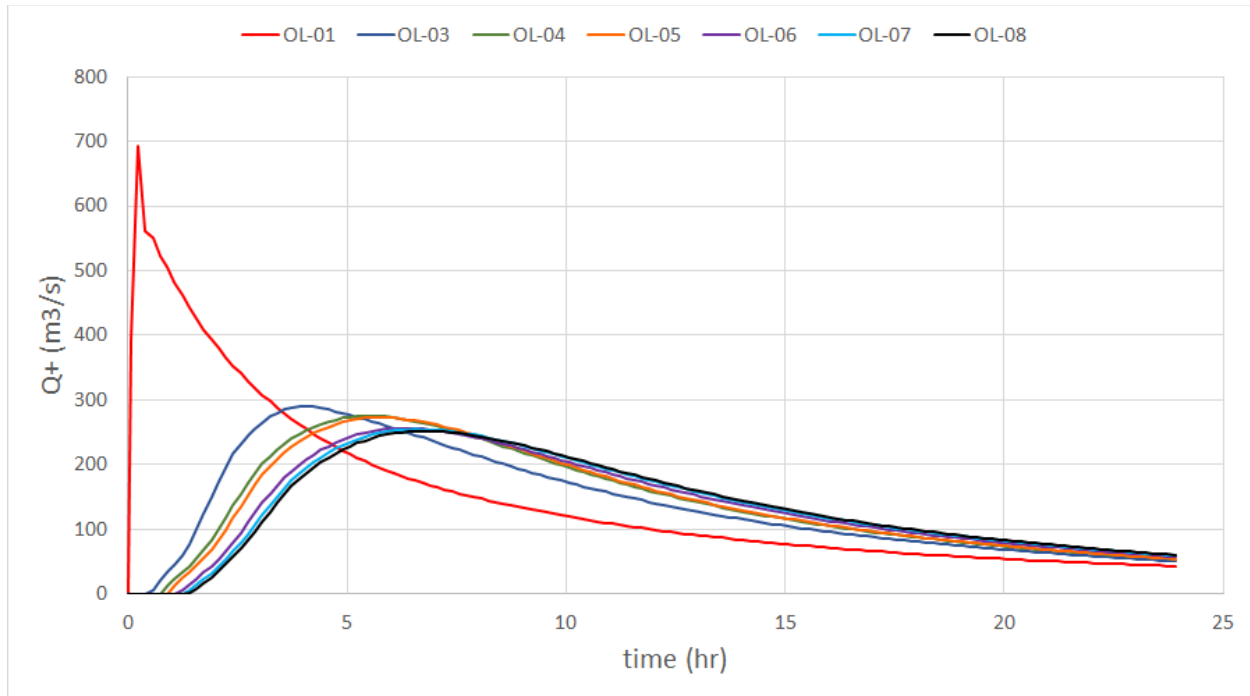
Figure 12 Hydrographs computed at observation lines 1, 3, 4, 5, 6, 7, and 8 for the Spillway Design Flood failure scenario (SDF).

6.2. Storm Surge Only (SSO) Simulation

Figure 13shows the maximum depth raster for the scenario SSO.
Figure 14 shows the flood arrival time raster for the scenario SSO.
Figure 15 shows the maximum flood discharge per unit width for the scenario SSO.

The discharge hydrographs computed at observation lines 1, 3, 4, 5, 6, 7, and 8 are plotted together in Figure 16. Due to tidal effect, the discharges alternate between negative (flow towards inland) and positive (flow towards the sea) values. The scenario SSO was is computed using the initial and boundary conditions taken from the storm surge simulation using CCHE2D (see Sections 2.2 and 2.3 of the report). Thus it basically repeats the same storm surge simulation using DSS-WISE™ software. Figure 17 compares the inundation areas computed using DSS-WISE™ with the original simulation obtained using CCHE2D. As it can be seen the agreement is quite good and the storm surge simulation with DSS-WISE™ yields the same storm surge flooding levels as in the simulation with CCHE2D.
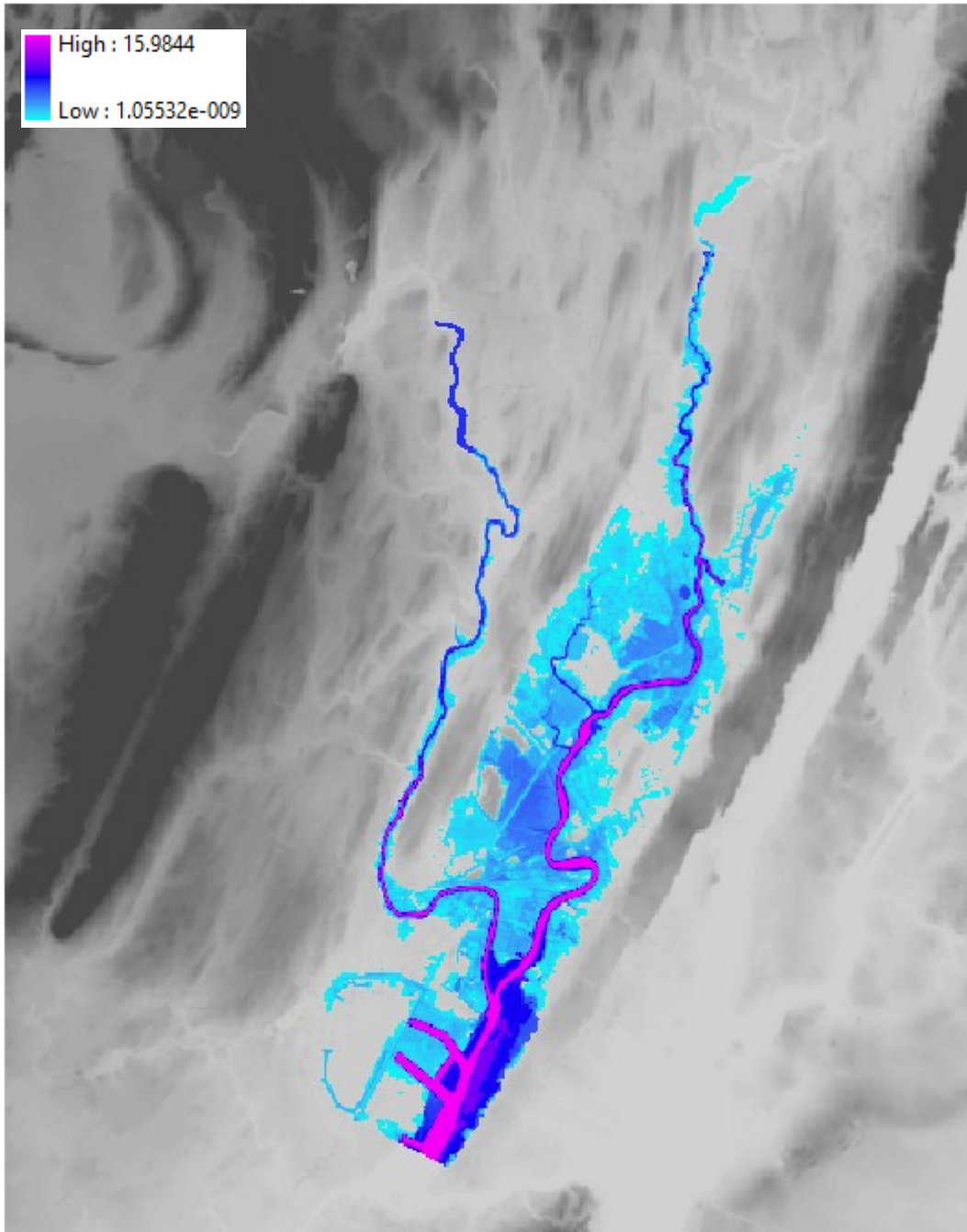
Figure 13 Map of maximum flow depths for the storm surge only scenario (SSO) as computed by DSS-WISE. The units for the legend are in meters.
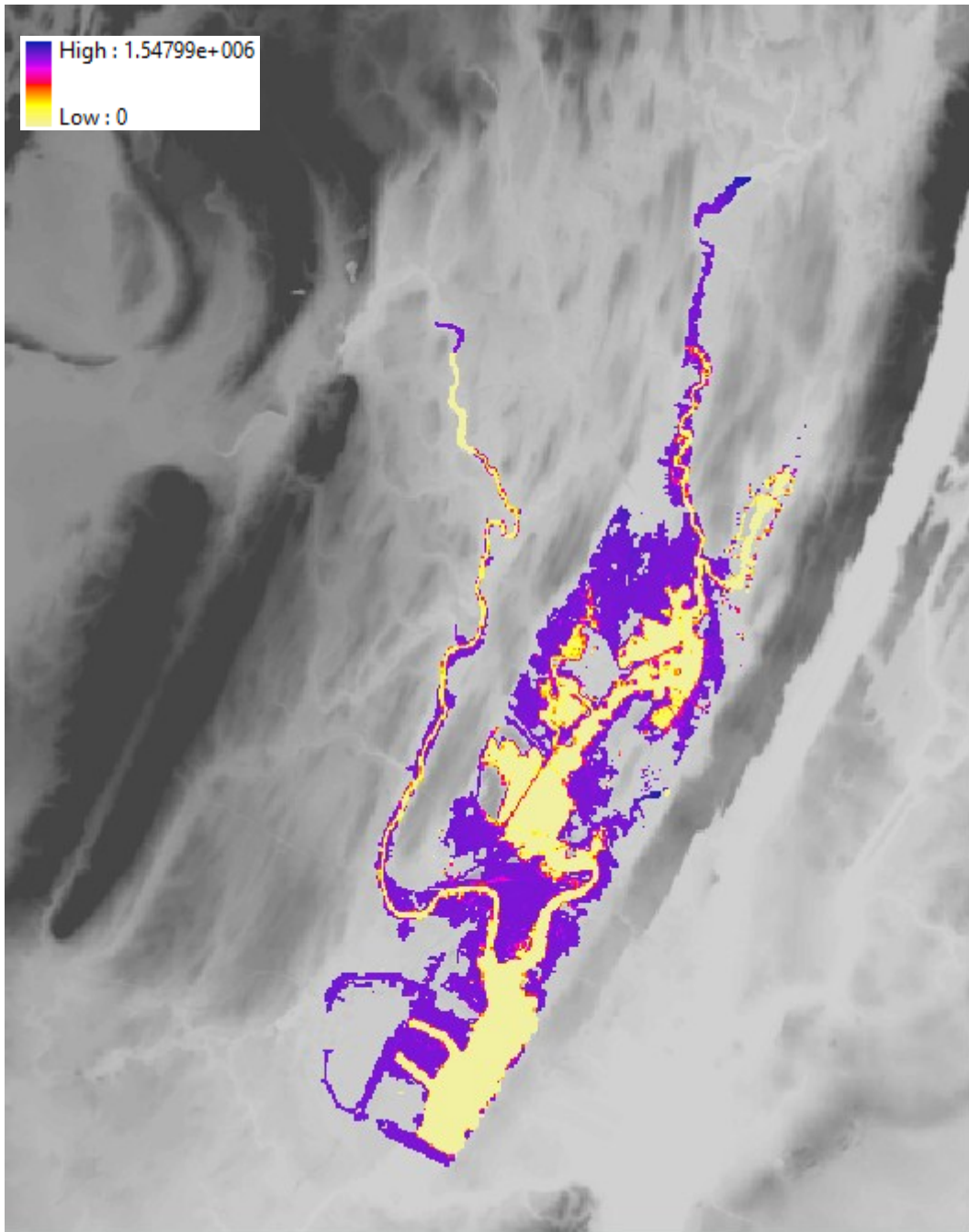
Figure 14 Map of flood arrival times for the storm surge only scenario (SSO) as computed by DSS-WISE. The units for the legend are in seconds.
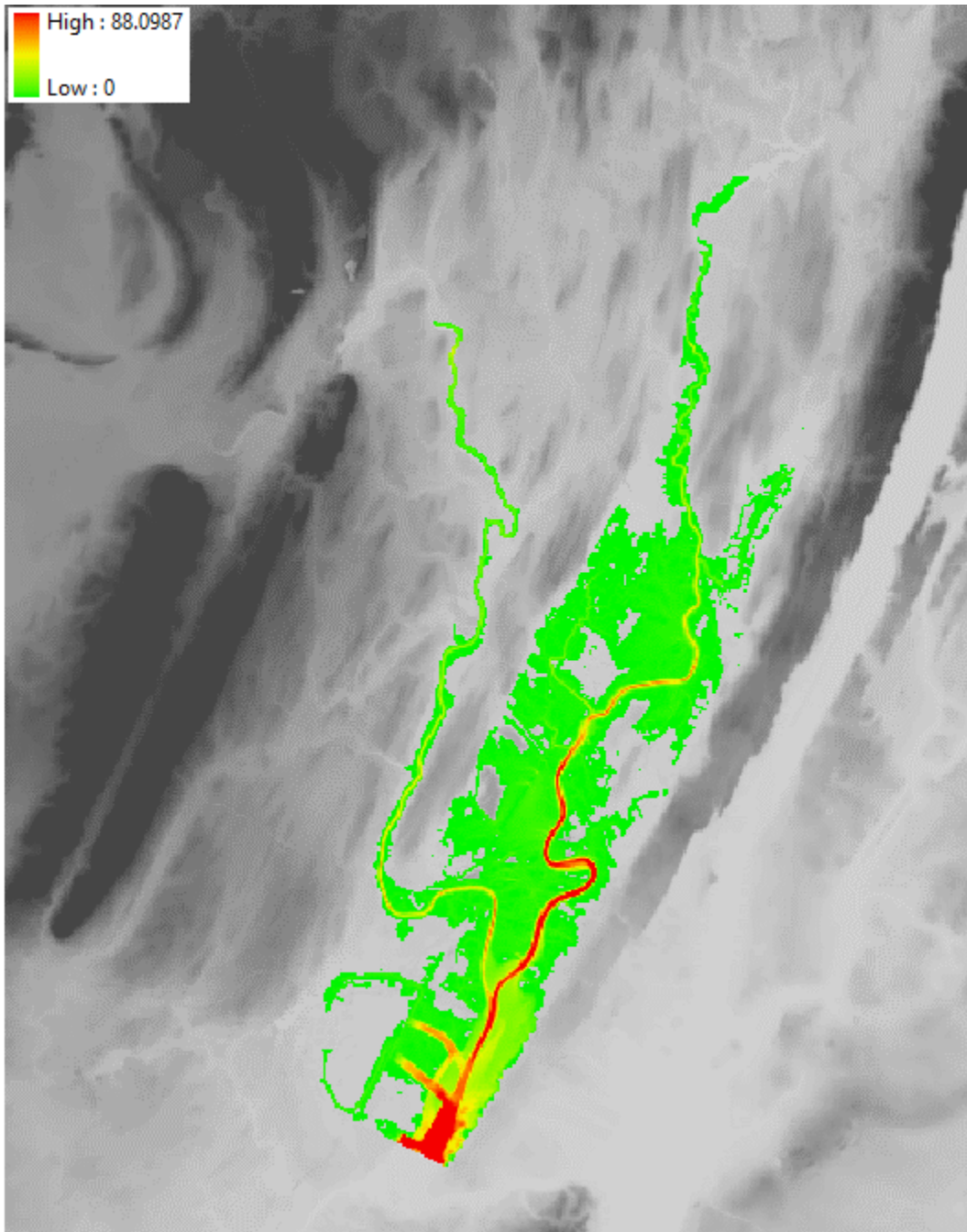
Figure 15 Map of maximum flow discharge per unit width for the storm surge only scenario (SSO) as computed by DSS-WISE. The units for the legend are in m^3/s/m.
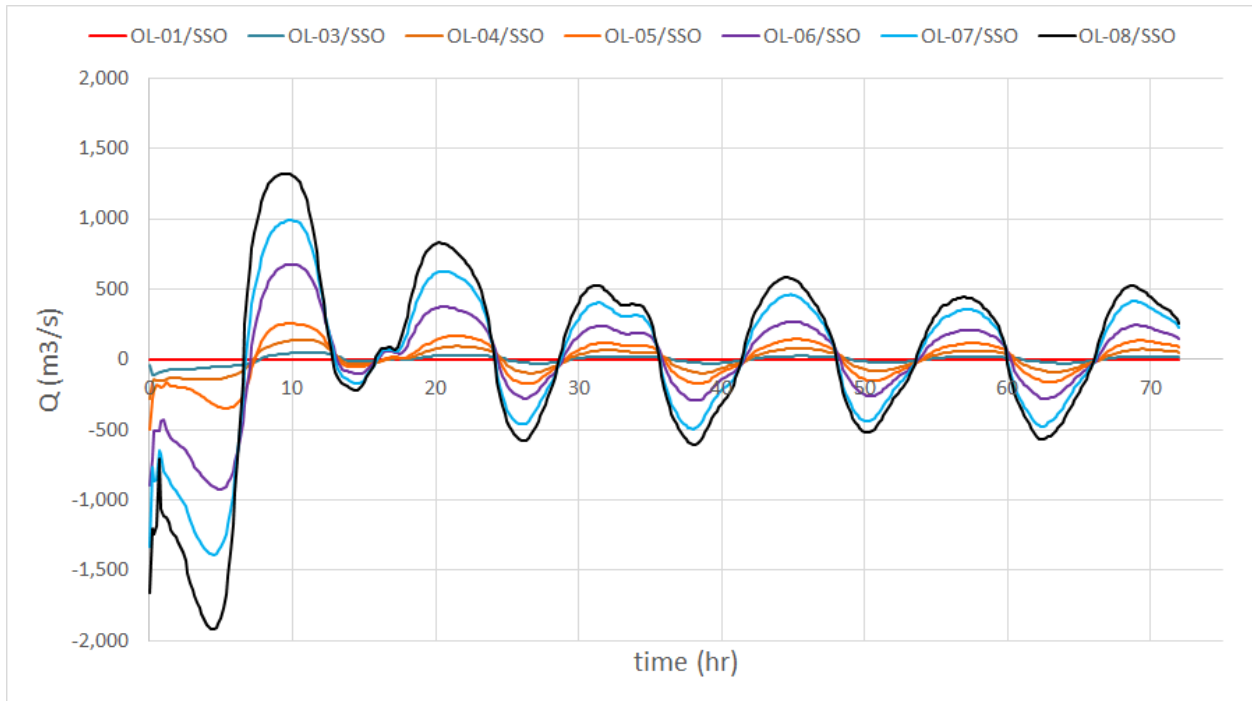
Figure 16 Hydrographs computed at observation lines 1, 3, 4, 5, 6, 7, and 8 for the Storm Surge Only (SSO) scenario.
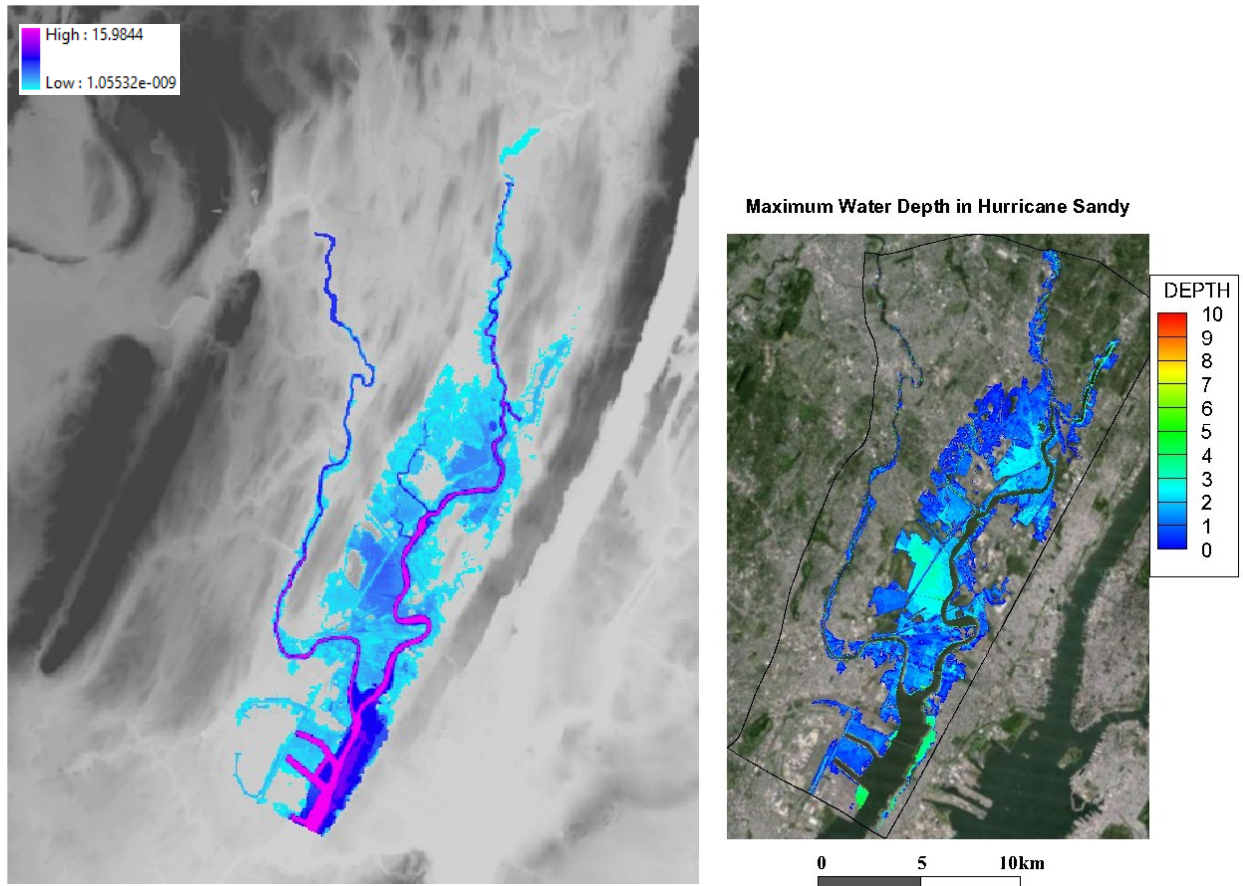
Figure 17 Inundation area and maximum flood depths computed with DSS-WISE™ (Left) and CCHE2D (Right). Although the color schemes are different, one can qualitatively see that, as expected, they are giving approximately similar results.

6.3. Dam-Break Failure during Storm Surge (DB&SS) Simulation

Figure 18 shows the maximum depth raster for the scenario DB&SS.
Figure 19 shows the flood arrival time raster for the scenario DB&SS.
Figure 20 shows the maximum flood discharge per unit width for the scenario DB&SS.

The discharge hydrographs computed at observation lines 1, 3, 4, 5, 6, 7, and 8 are plotted together in Figure 21. The maximum discharge of $773m^3/s$ is observed at OL-01 at 0.5 hours after the initiation of the breach. The discharge at OL-01 rises very quickly but decays more slowly. The discharge at OL-01 is not affected by the tidal effect and the flow remains positive (i.e. towards downstream) throughout the entire simulation duration and does not show any fluctuations. The discharge on all other stations are affected by the tidal fluctuations. As expected the influence of the tidal fluctuations increases from OL-02, which is closer to the dam, to OL-08, which is closer to the seashore. At station OL-02, when the dam-break flood arrives the flow discharge is towards inland. The discharge due to dam-break flood arriving at OL-02 reverses the direction of the flow towards downstream and remains strong enough to keep it positive throughout the simulation. In other stations (from OL-03 to OL-08), the dam-break flow is not strong enough to significantly affect the flows due to tide and storm surge. The hydrographs for OL-03 to OL-08 clearly show a discharge changing direction under the tidal effects.
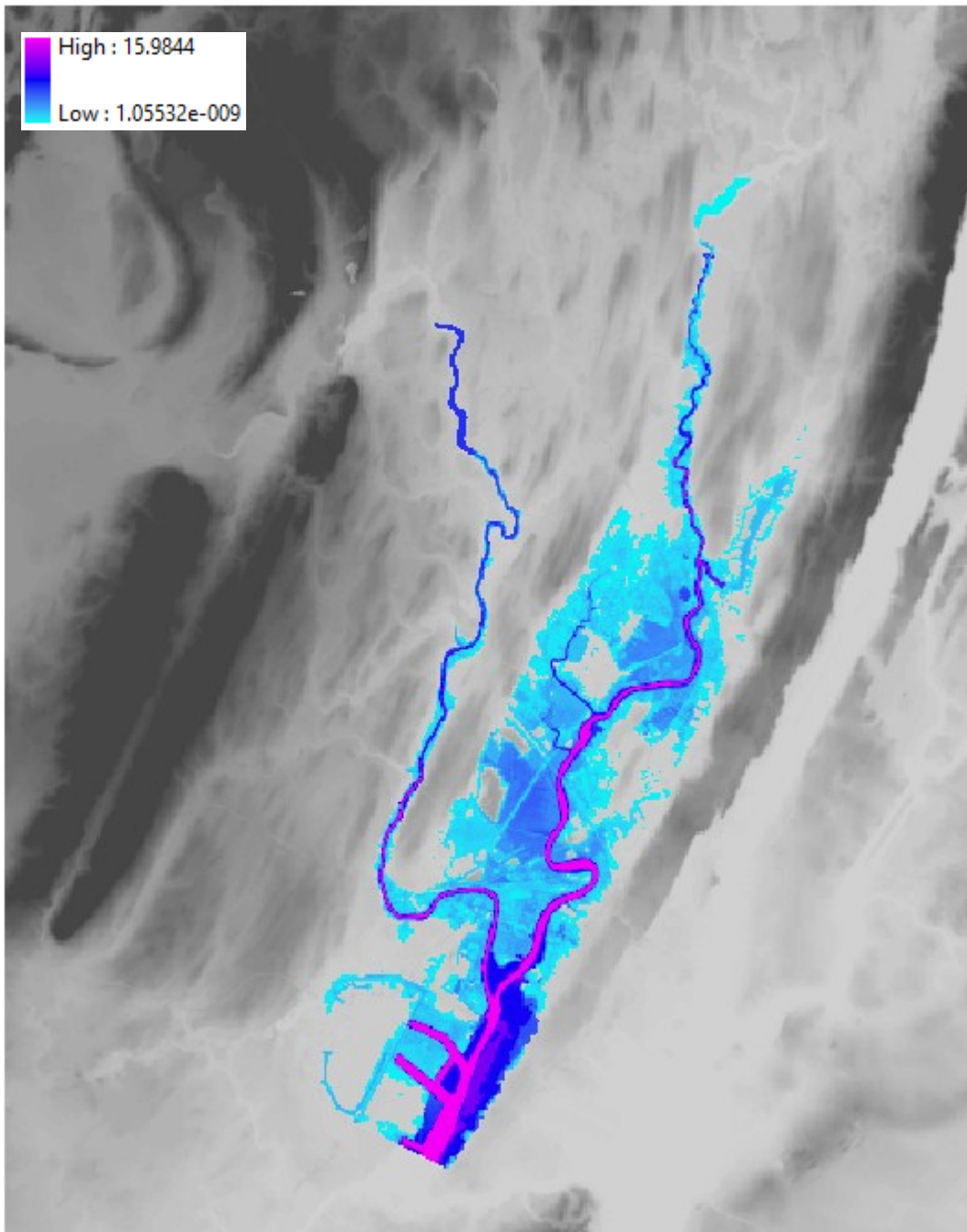
Figure 18 Map of maximum flow depths for the Dam-Break during Storm Surge scenario (DB&SS). The units for the legend are in meters.
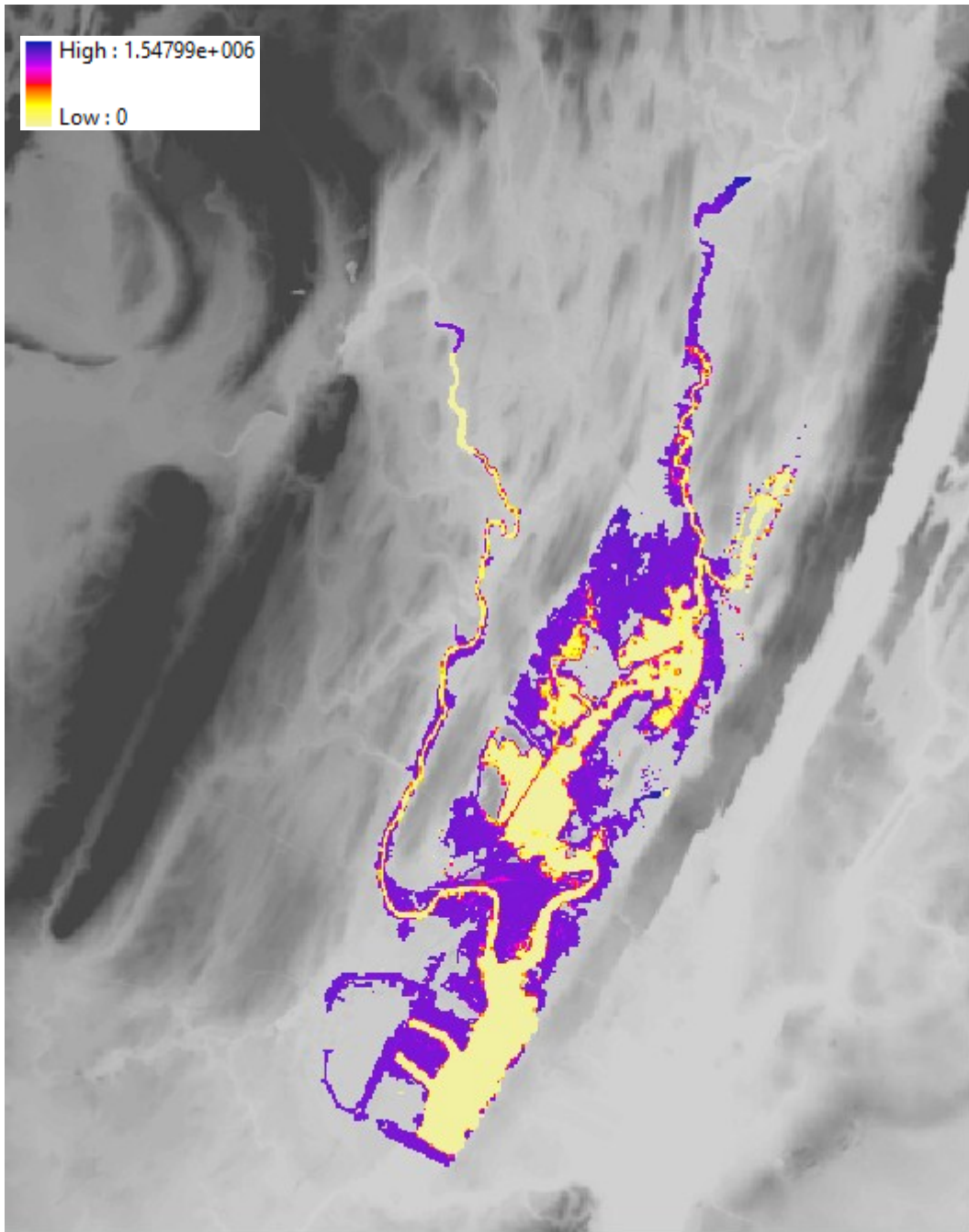
Figure 19 Map of flood arrival times for the Dam-Break during Storm Surge scenario (DB&SS). The units for the legend are in seconds.
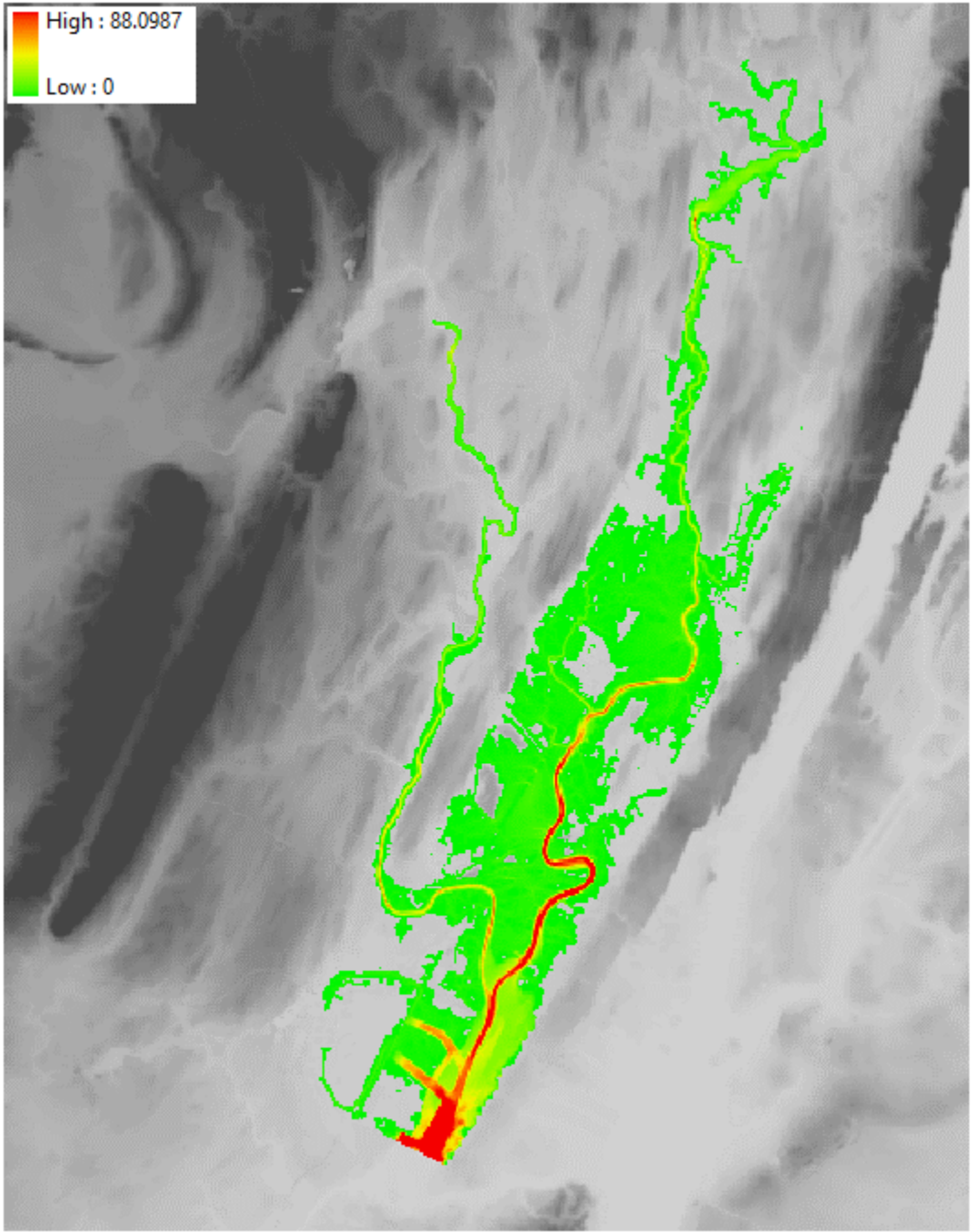
Figure 20 Map of maximum flow discharge per unit width for the Dam-Break during Storm Surge scenario (DB&SS). The units for the legend are in $m^3/s/m$.
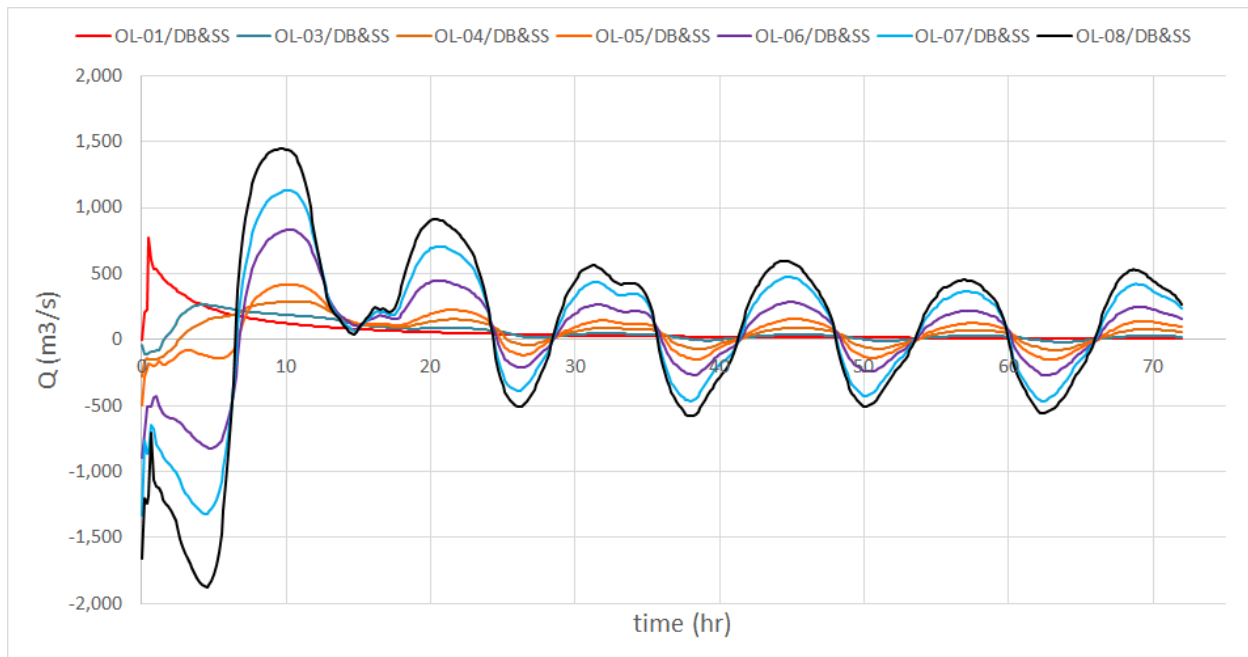
Figure 21 Hydrographs computed at observation lines 1, 3, 4, 5, 6, 7, and 8 for the Dam-Break during Storm Surge (DB&SS) scenario.

7. Discussion of Simulation Results

The comparison of discharges computed at observation lines OL-01 through OL-08 (with the exception of OL-02[6]) and the water surface elevations computed at observation stations OP-01 through OP-25 for the three scenarios simulated, i.e. Spillway Design Flood failure (SDF, blue line), Storm Surge Only (SSO, orange line) and Dam-Break during Storm Surge (DB&SS, red line) can provide an understanding with regard to the additional level of damage and risk due to the hypothetical failure of Oradell Dam during a Hurricane Sandy-like storm surge as represented by the base line scenario.

Computed discharges crossing observation lines OL-01 to OL-08 are plotted in Figure 22 through Figure 28 for all three scenarios: Spillway Design Flood failure (SDF, blue line), Storm Surge Only (SSO, orange line) and Dam-Break during Storm Surge (DB&SS, red line). Based on these plots, the following observations can be made:

- The discharge across OL-01 (Figure 22) is practically not influenced by the storm surge. The discharge hydrographs for the scenarios SDF (blue line) and DB&SS (red line) are almost the same and the discharge for the scenario SSO (orange line) is null.
- The study of the discharge hydrographs for the scenario SSO (orange line) shows that the storm surge reaches observation lines OL-03 through OL-08 (see Figure 23 through Figure 28).
- Referring to Figure 23, for the scenario DB&SS (red line) the dam-break flood arrives at the observation line OL-03 1.17hr after the failure of the dam when the storm surge is advancing inland (orange line is negative). Until that time the red line and orange line are the same. After t=1.17hr the red line begins to diverge from the orange line and the discharge increases due to the dam-break flood. The dam-break flood becomes the dominant discharge and the red line

---

[6] OL-02 is not used due to the fact that the eastern end of the observation line crosses a meander of the river in both directions.

approaches the blue line. As the dam-break flood discharge decreases, the red line begins to approach the orange line. About 55hr after the dam-break the red and orange lines are the same.
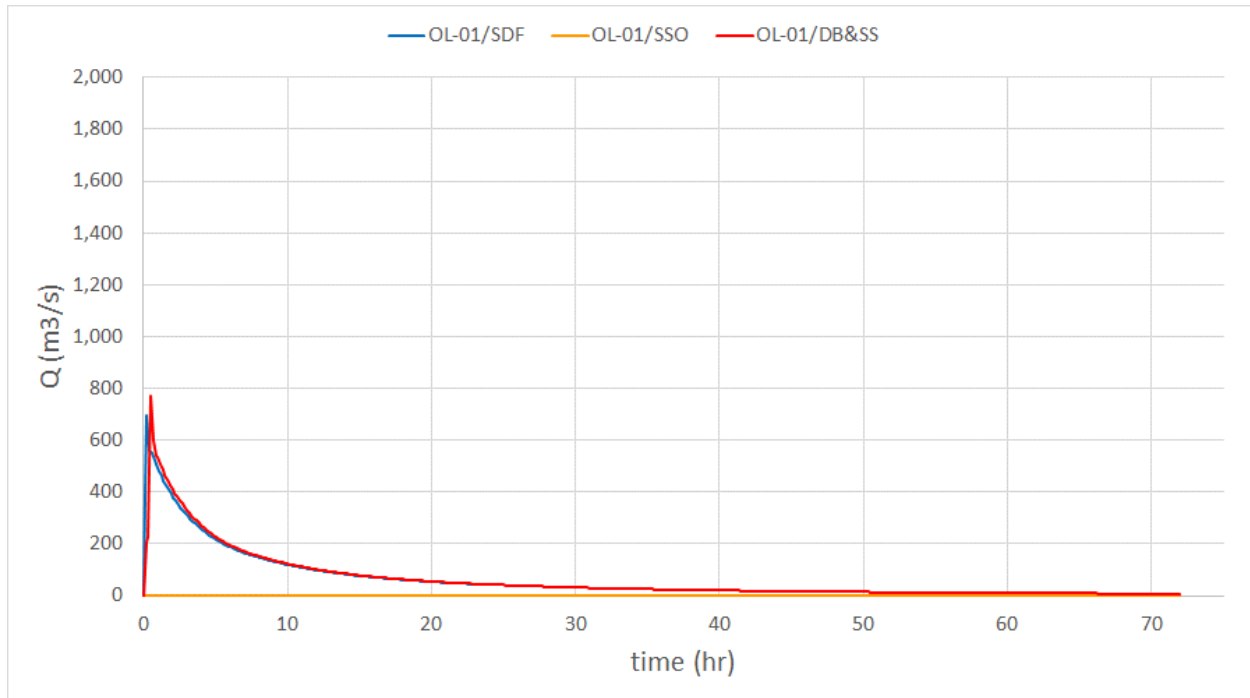
Figure 22 Comparison of computed discharges crossing observation line OL-01.

- Similarly, the differences between red and orange lines in Figure 24 through Figure 28 are also due to the dam-break flood discharges. The influence of the dam-break flood discharge is greatest for the observation line closest to the dam (OL-03) and decreases with downstream distance due to attenuation. The differences are the smallest for the observation line OL-08, which is farthest downstream. Moreover, the duration during which the dam-break flood influences the discharge decreases with downstream distance from the dam. Observation of plots in Figure 23 through Figure 28 shows that the time at which the red and orange line begin to merge again is about 55hr for OL-03 whereas at OL-08 it is about 41hr.
- It is also important to note that, at observation lines OL-04 through OL-08 (Figure 24 through Figure 28) the discharge for the scenario DB&SS (red line) remains positive (towards downstream of the dam) during the first 24 hours, approximately, after the dam break whereas the discharge for the scenario SSO (orange line) at times reverses direction to become negative (i.e. towards the dam). It is the dam-break flood discharge that counters the inland movement of the storm surge flood and forces the discharge across these observation lines to remain positive.
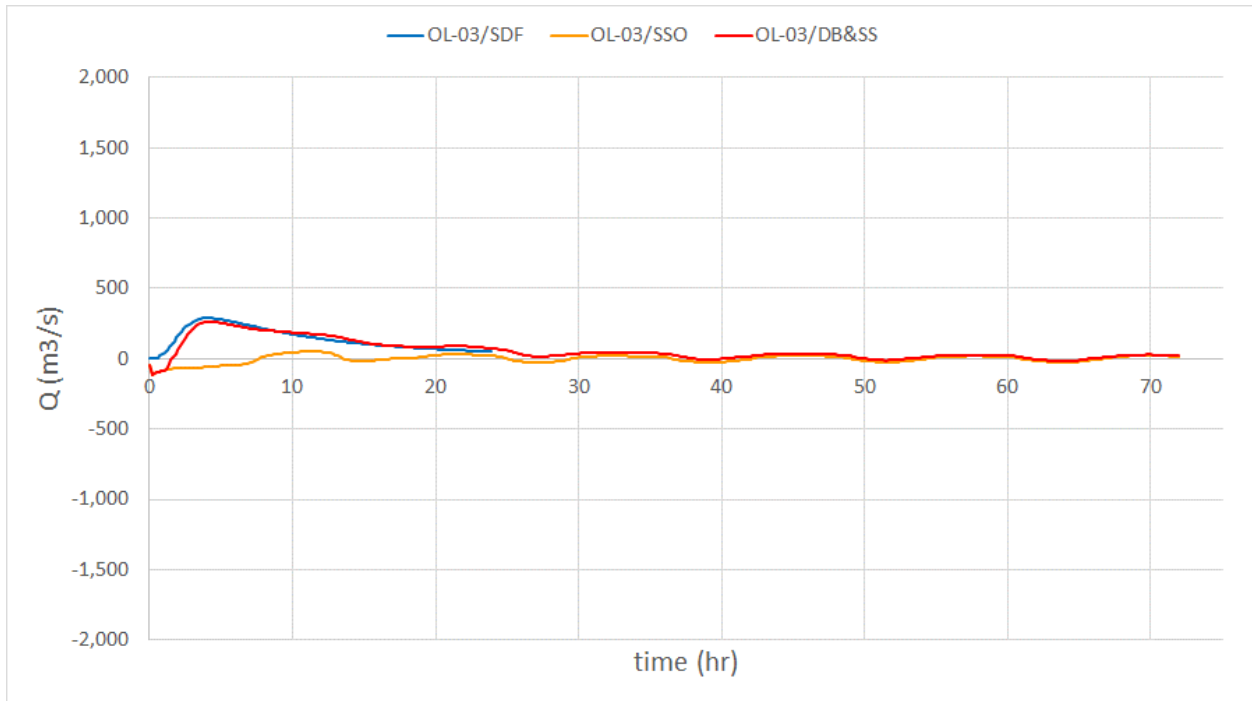
Figure 23 Comparison of computed discharges crossing observation line OL-03.
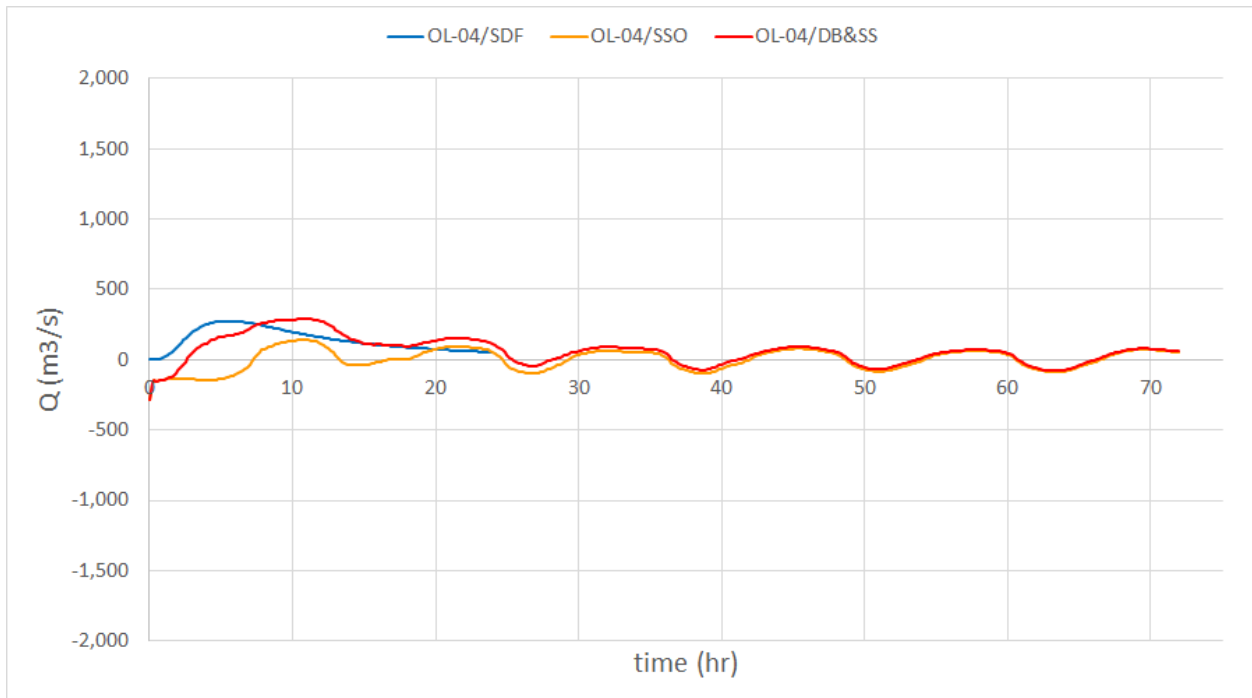
Figure 24 Comparison of computed discharges crossing observation line OL-04.
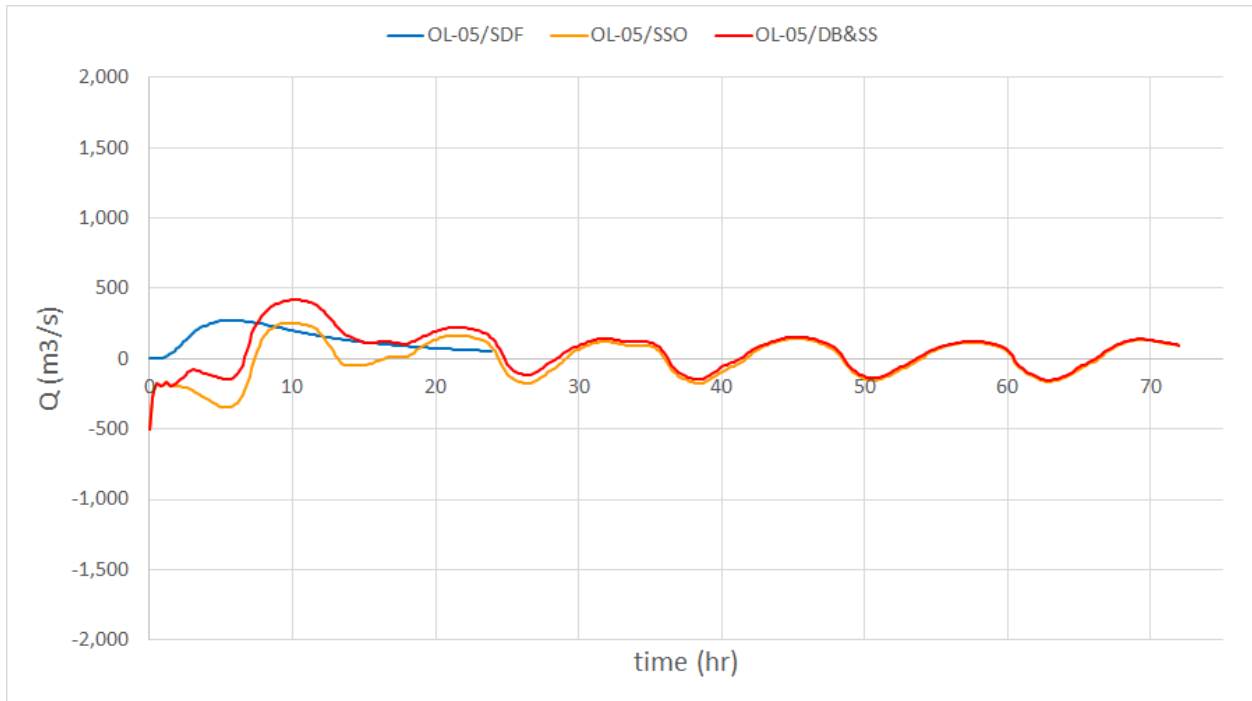
Figure 25 Comparison of computed discharges crossing observation line OL-05.
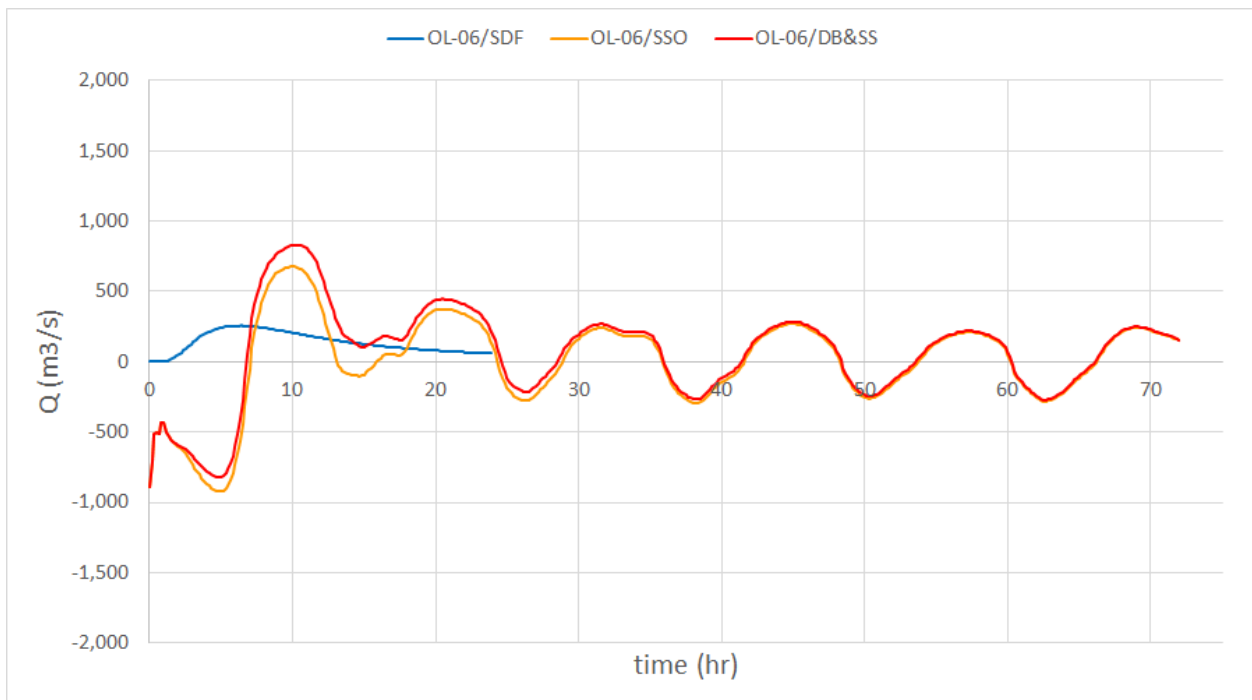
Figure 26 Comparison of computed discharges crossing observation line OL-06.
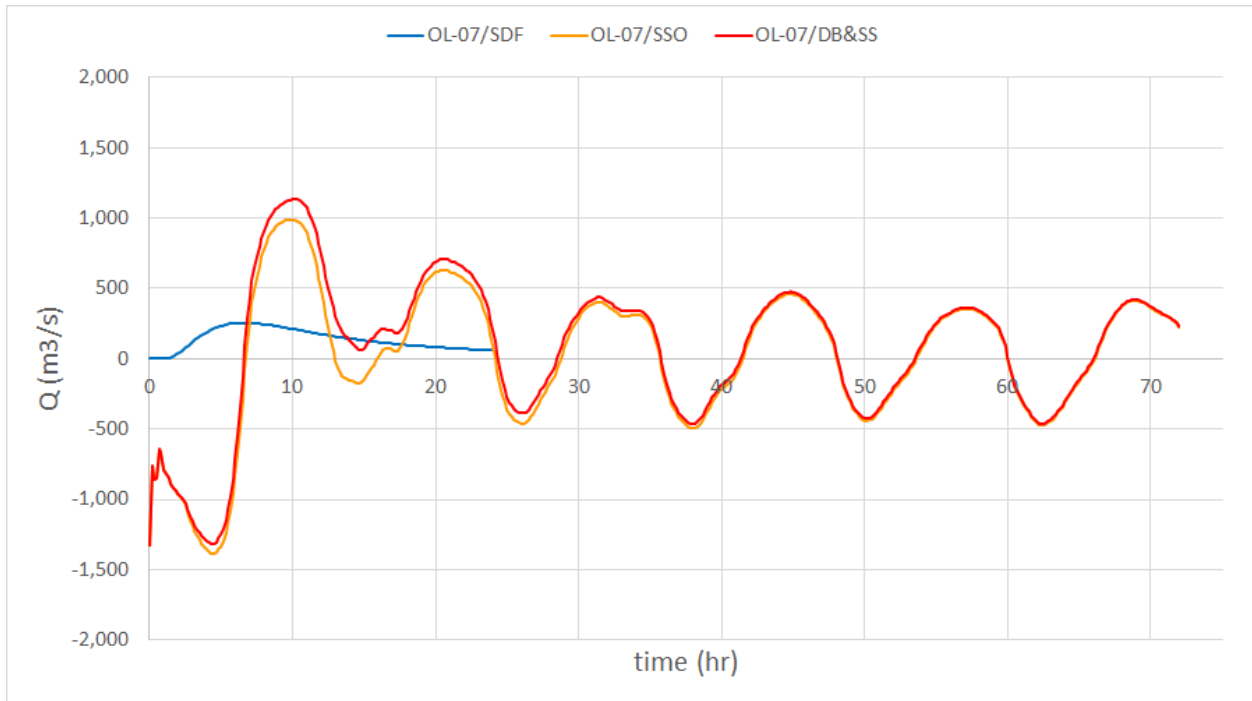
Figure 27 Comparison of computed discharges crossing observation line OL-07.
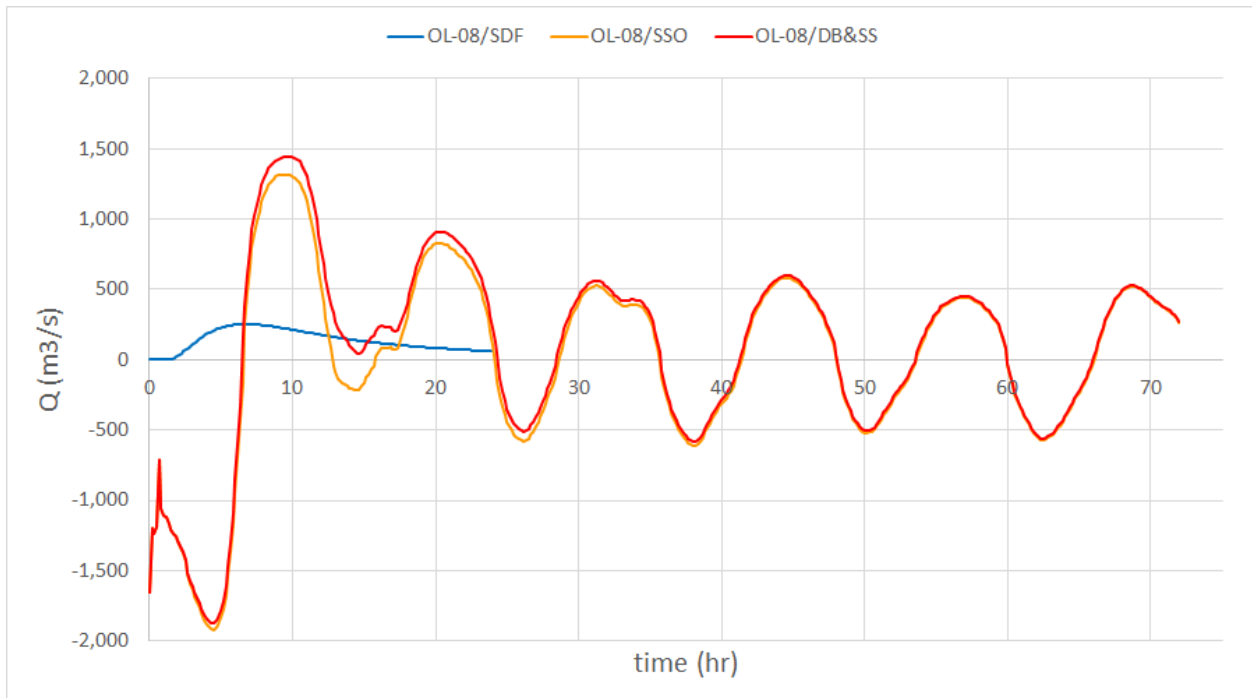
Figure 28 Comparison of computed discharges crossing observation line OL-08.

Water surface elevations computed at observation points OP-01 to OP-25 are plotted in Figure 29, Figure 30, Figure 31, and Figure 32 for all three scenarios Spillway Design Flood failure (SDF, blue line), Storm

Surge Only (SSO, orange line) and Dam-Break during Storm Surge (DB&SS, red line). On each figure the bed elevation corresponding to the observation point is plotted as a horizontal line (black line). The following observations can be made:

- Blue line (SDF) and red line (DB&SS) at observation points OP-01, OP-02 and OP-03 (Figure 29) are almost the same indicating that, at these stations, the hydrograph resulting from dam-break is not influenced by the storm surge. This observation is also corroborated by the fact the orange line (SSO) is the same as the black line corresponding to ground elevation, z_b.

- Stations from OP-04 to OP-25 are influenced by storm surge. Comparison of red line red line (DB&SS) and orange line (SSO) shows that, at stations OP-04 to OP-10 the red line is higher than the orange line. The water surface elevation difference between the red line and orange line is due to the dam-break flood discharge. As it can be seen, the influence of the dam-break flood is the largest at OP-04 and decreases towards downstream. At OP-10, the influence of the dam-break flood becomes negligible. It can also be seen that, at a given station, the influence of the dam-break flood decreases with time, which is expected since dam-break is an impulse type wave. The dam-break flood influences the water surface elevations at OP-04 for the first 55 hours following the dam break whereas at OP-08, the influence is significant only for the first 25 hours. As the influence of the dam-break flood becomes negligible at a given station, red (DB&SS) and orange (SSO) lines become almost the same.

- At observation points OP-13 to OP-25 (Figure 30, Figure 31 and Figure 32), the red (DB&SS) and orange lines (SSO) are practically the same. This indicates that the influence of the dam-break flood is negligible or nonexistent. This is also corroborated by the fact that the blue line (SDF) is the same as the black line corresponding to ground elevation, z_b.
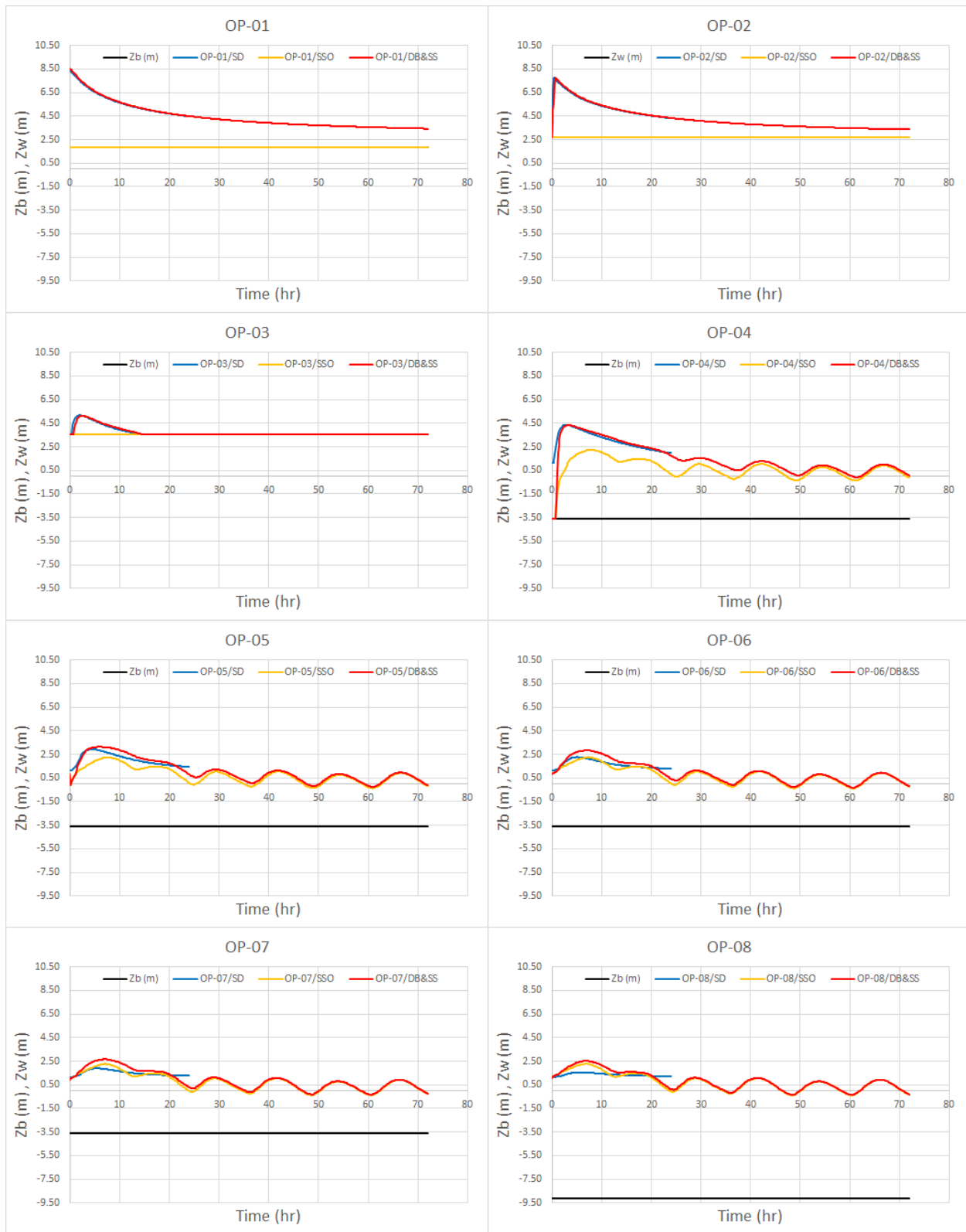
Figure 29 Comparison of water surface elevations computed at observation points OP-01 to OP-08 for the scenarios SDF, SSO and DB&SS.
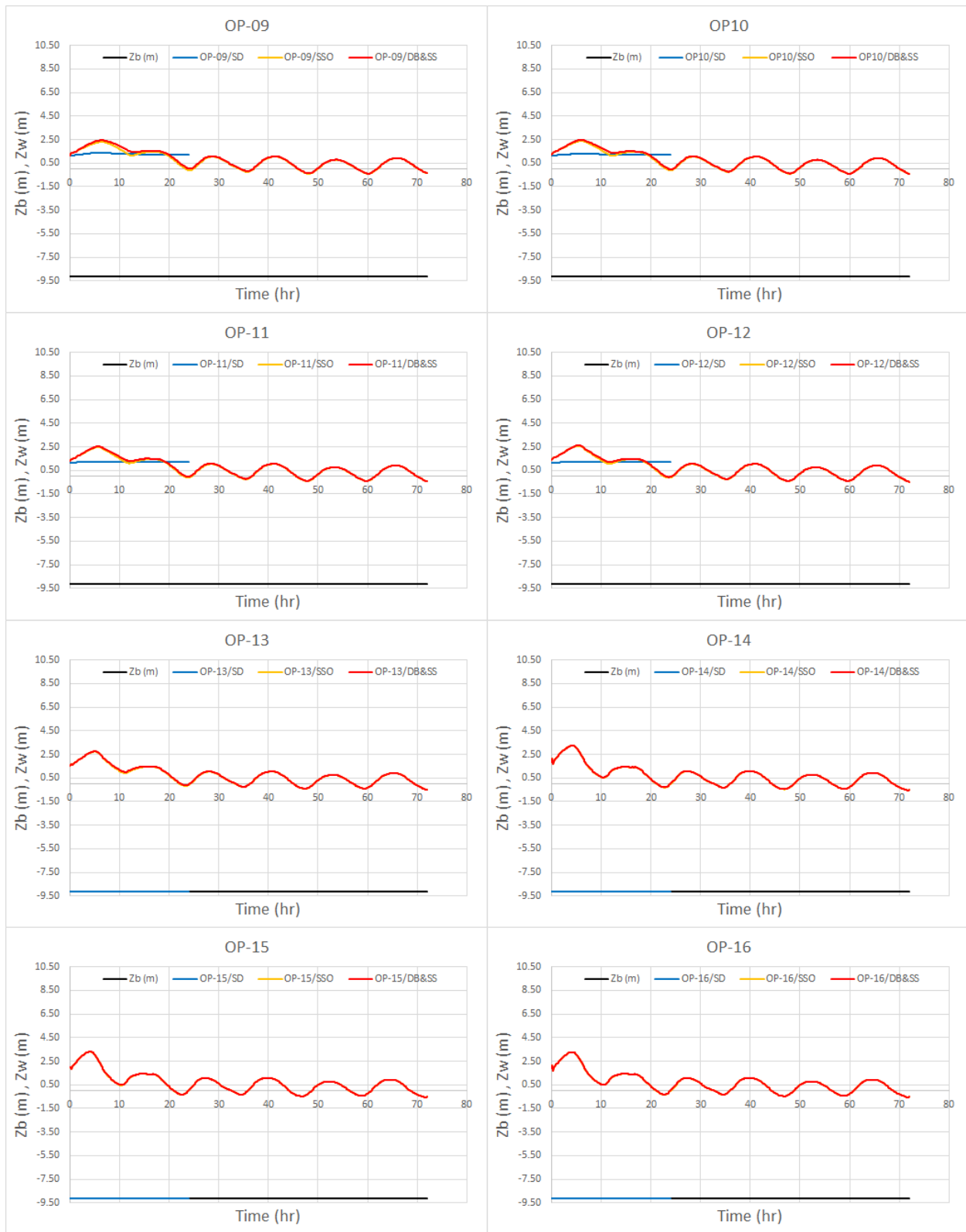
Figure 30 Comparison of water surface elevations computed at observation points OP-09 to OP-16 for the scenarios SDF, SSO and DB&SS.
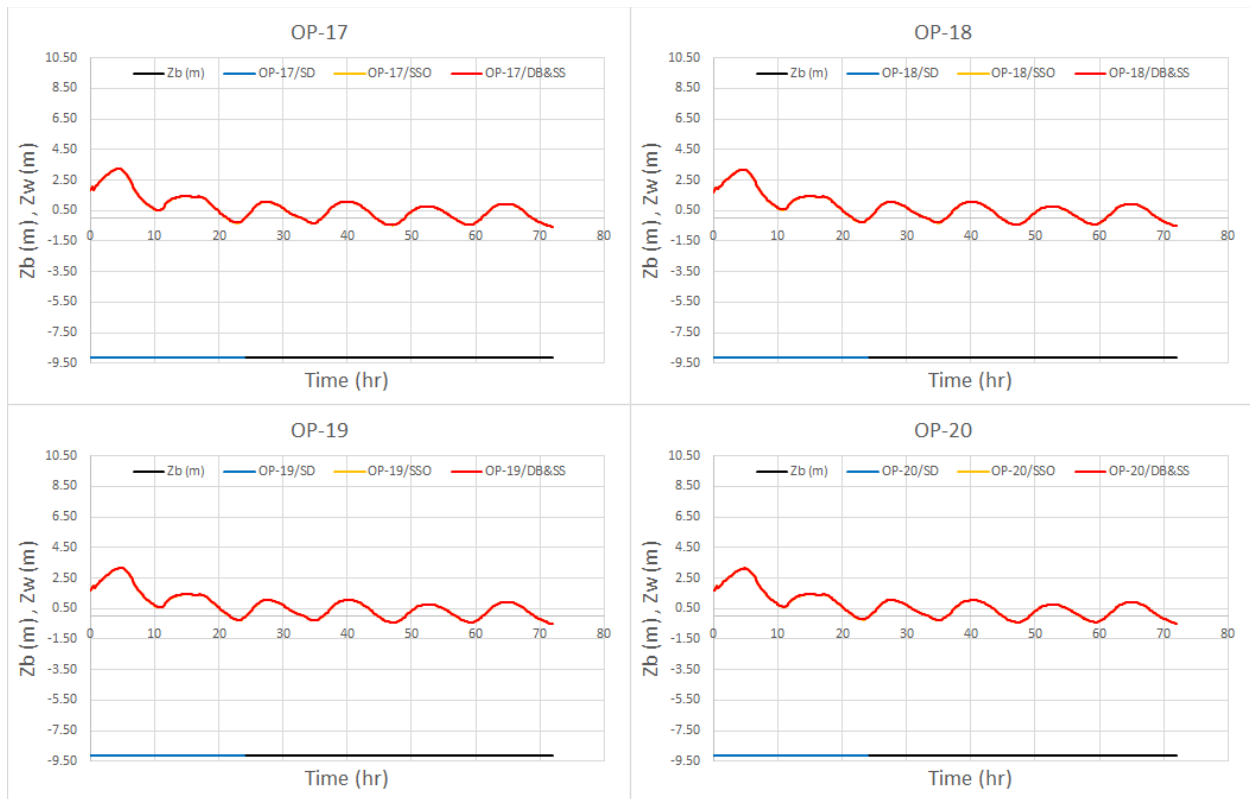
Figure 31 Comparison of water surface elevations computed at observation points OP-17 to OP-20 for the scenarios SDF, SSO and DB&SS.
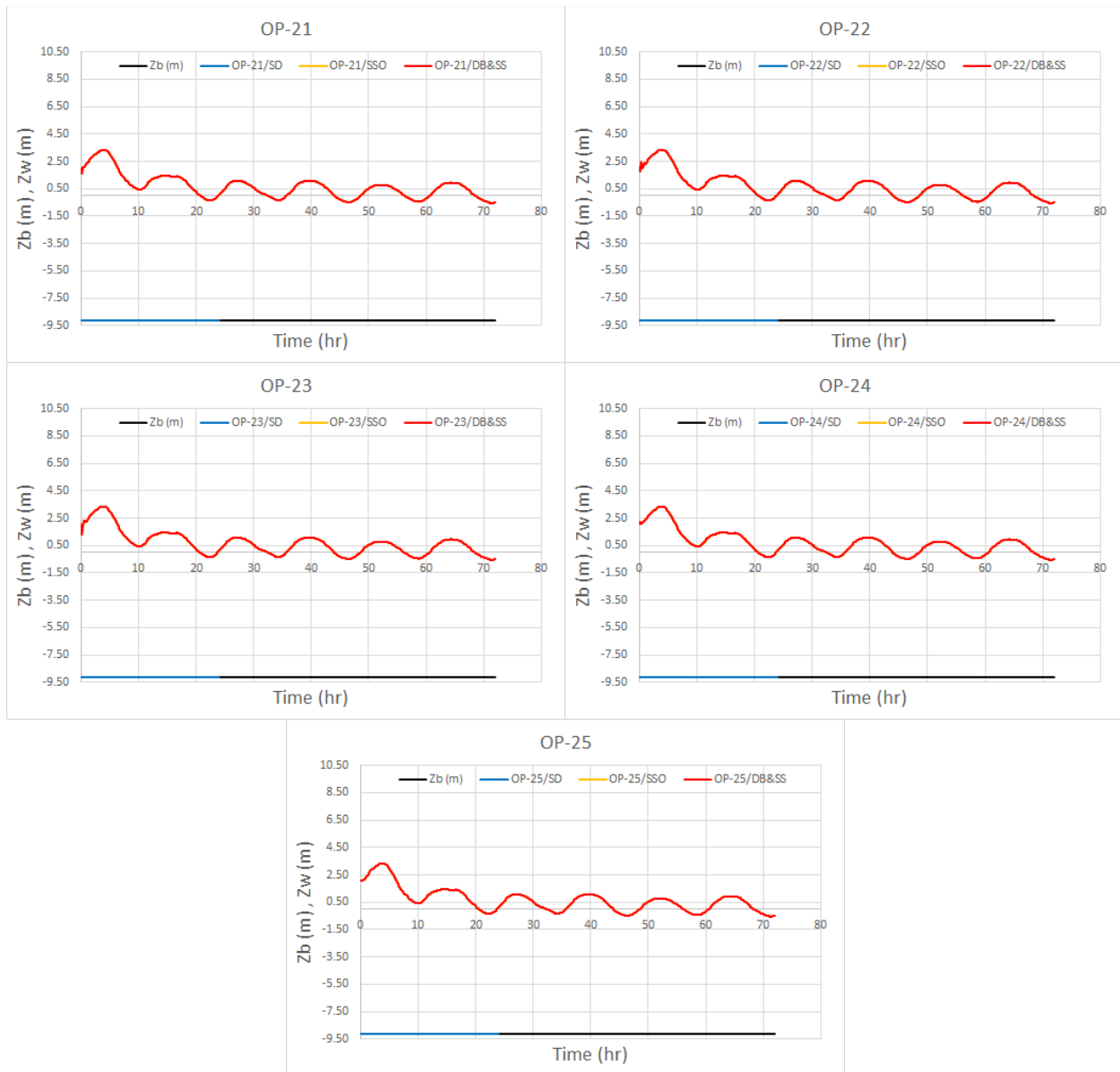
Figure 32 Comparison of water surface elevations computed at observation points OP-21 to OP-25 for the scenarios SDF, SSO and DB&SS.

Figure 33 shows the raster map of differences in maximum flood depth between the scenarios DB&SS and SSO. It was generated by subtracting the maximum flood depths computed for the scenario SSO from those computed for the scenario DB&SS. As it can be seen the differences in maximum flow depth decrease with downstream distance from the dam. Near the observation point OP-05, it is about 1m and reduces to about 0.10m near OP-10. Downstream of OP-10, the differences are generally not significant.

A similar trend is also observed in Figure 34, which shows the differences in maximum flow discharge per unit width, which was generated by subtracting the maximum flood discharges per unit width computed for the scenario SSO from those computed for the scenario DB&SS.
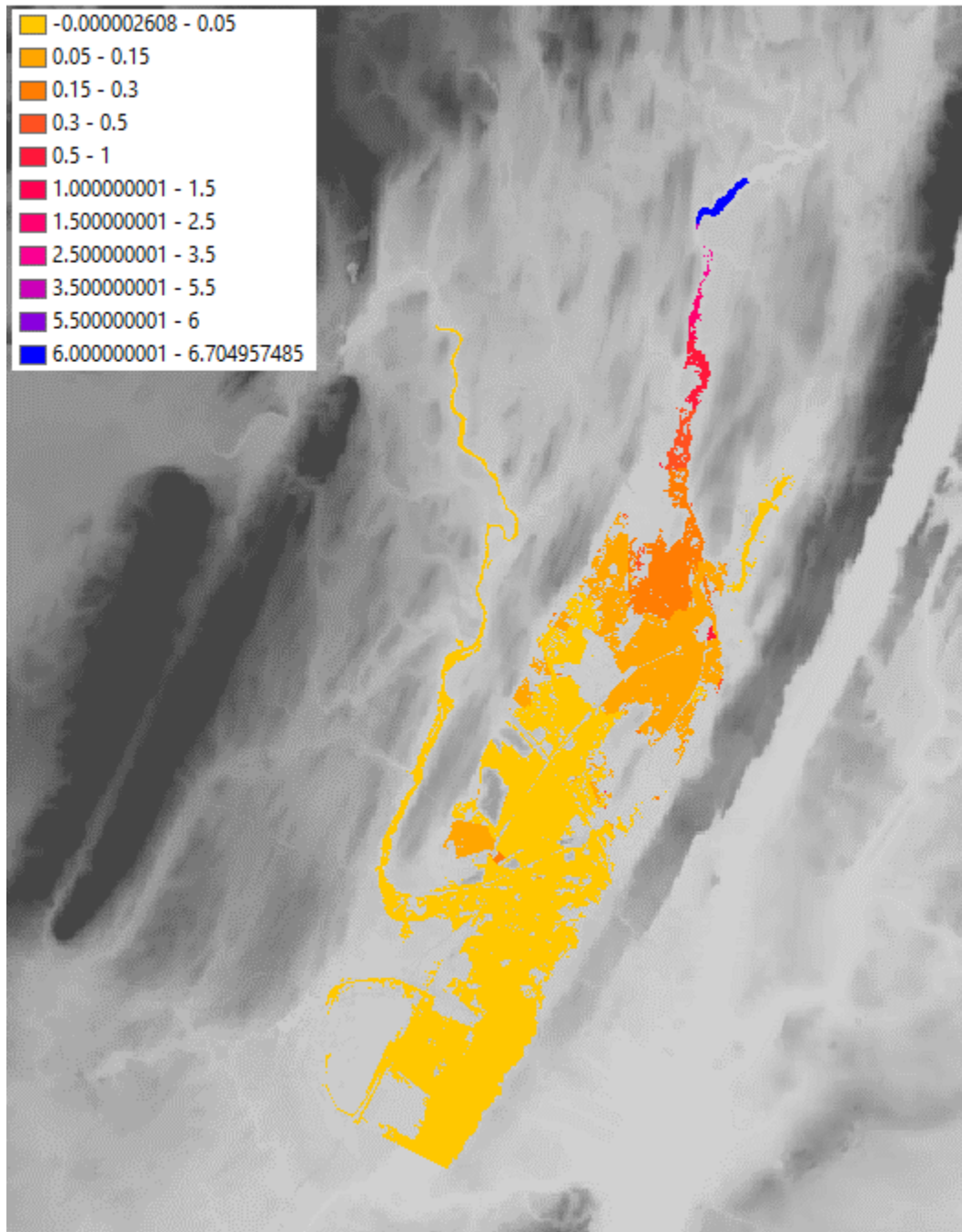
Figure 33 Differences in computed maximum flow depths (h_{max} for DB&SS - h_{max} for SSO). The units for the legend are in m.
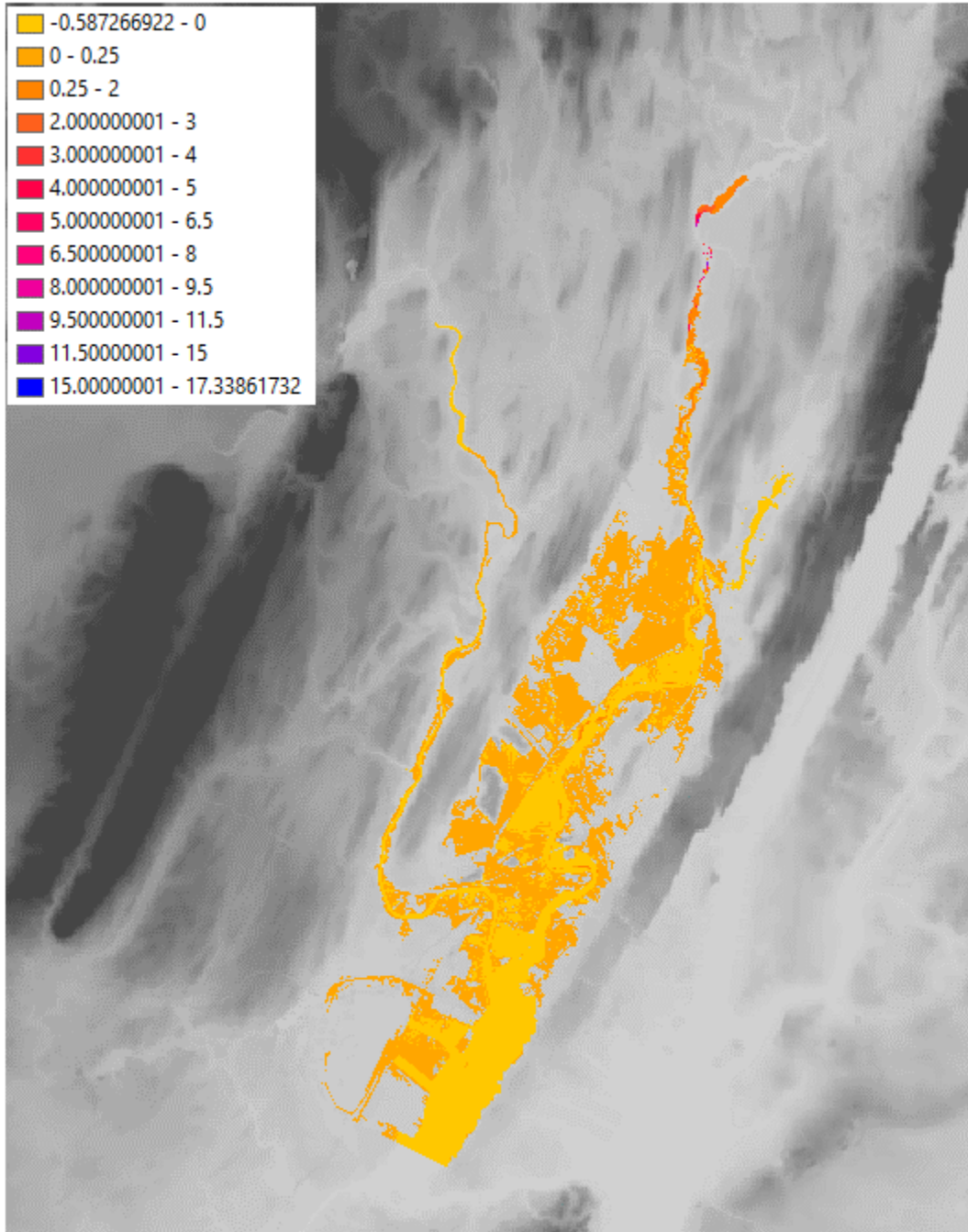
Figure 34 Differences in computed maximum flow discharge per unit width (q_{max} for DB&SS - q_{max} for SSO). The units for the legend are in $m^3/s/m$.

REFERENCES

Altinakar, M.S., McGrath, M.Z., Ramalingam, V.P. and Omari, H. 2010. "2D Modeling of Big Bay Dam Failure in Mississippi: Comparison with Field Data and 1D Model Results"; *Proceedings of the International Conference on Fluvial Hydraulics (River Flow 2010)*, September 8-10, Braunschweig, Germany.

Altinakar, M.S., McGrath, M.Z., Matheu, E.E., Ramalingam, V.P., Seda-Sanabria, Y., Breitkreutz, W., Oktay, S., Zou, J., & Yezierski, M. 2012a. Validation of Automated Dam-Break Flood Simulation Capabilities and Assessment of Computational Performance. *Proc. of Dam Safety 2012 Conf.*, *ASDSO*, Sep. 16-21, 2012, Denver, CO.

Altinakar, M.S. and McGrath, M.Z. 2012b. "Parallelized Two-Dimensional Dam-Break Flood Analysis with Dynamic Data Structures," *ASCE-EWRI, 2012 World Environmental & Water Resources Congress*, Albuquerque, New Mexico, May 20–24, 2012.

Godunov, S.K. 1959. A Difference Scheme for Numerical Solution of Discontinuous Solution of Hydrodynamic Equations. *Math. Sbornik, 47, 271–306, transl. US Joint Publ. Res. Service, JPRS 7226, 1969*.

Godunov S.K., Zabrodine, A., and Ivanov, A. 1976. "Résolution numérique des problèmes multidimensionnels de la dynamique des gaz," *Editions MIR de Moscou,* 1976.

Harten, A., Lax, P., and van Leer, D. 1983. "On Upstream Differencing and Godunov-type Methods for Hyperbolic Conservation Laws," *SIAM Review* 25, pp. 35–61.

Toro, E.F., Spruce, M., & Speares, W. (1992). Restoration of the Contact Surface in the HLL–Riemann Solver, *Technical Report CoA–9204, Department of Aerospace Science, College of Aeronautics, Cranfield Institute of Technology, UK*.

Toro, E. F., Spruce, M., Speares, W. 1994. "Restoration of the contact surface in the HLL-Riemann Solver," *Shock Waves*, 4(1), pp. 25–34.